IEC TS 62997

Edition 1.0 2017-06

TECHNICAL SPECIFICATION

colour inside

Industrial electroheating and electromagnetic processing equipment – Evaluation of hazards caused by magnetic nearfields from 1 Hz to 6 MHz

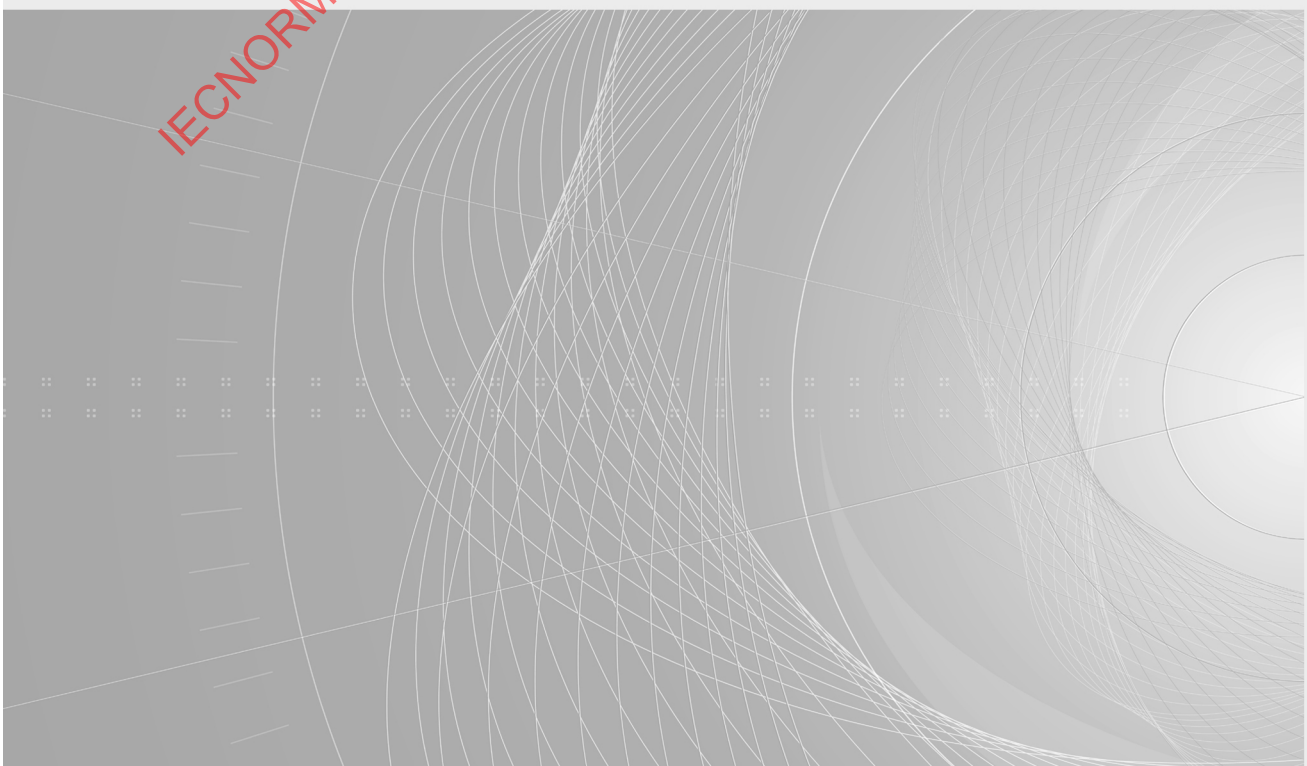

IEC TS 62997:2017-06(en)

IEC Central Office
3, rue de Varembé
CH-1211 Geneva 20
Switzerland

Tel.: +41 22 919 02 11
Fax: +41 22 919 03 00
info@iec.ch
www.iec.ch

About the IEC
The International Electrotechnical Commission (IEC) is the leading global organization that prepares and publishes International Standards for all electrical, electronic and related technologies.

About IEC publications
The technical content of IEC publications is kept under constant review by the IEC. Please make sure that you have the latest edition, a corrigenda or an amendment might have been published.

IEC Catalogue - webstore.iec.ch/catalogue
The stand-alone application for consulting the entire bibliographical information on IEC International Standards, Technical Specifications, Technical Reports and other documents. Available for PC, Mac OS, Android Tablets and iPad.

IEC publications search - www.iec.ch/searchpub
The advanced search enables to find IEC publications by a variety of criteria (reference number, text, technical committee,…). It also gives information on projects, replaced and withdrawn publications.

IEC Just Published - webstore.iec.ch/justpublished
Stay up to date on all new IEC publications. Just Published details all new publications released. Available online and also once a month by email.

Electropedia - www.electropedia.org
The world's leading online dictionary of electronic and electrical terms containing 20 000 terms and definitions in English and French, with equivalent terms in 16 additional languages. Also known as the International Electrotechnical Vocabulary (IEV) online.

IEC Glossary - std.iec.ch/glossary
65 000 electrotechnical terminology entries in English and French extracted from the Terms and Definitions clause of IEC publications issued since 2002. Some entries have been collected from earlier publications of IEC TC 37, 77, 86 and CISPR.

IEC Customer Service Centre - webstore.iec.ch/csc
If you wish to give us your feedback on this publication or need further assistance, please contact the Customer Service Centre: csc@iec.ch.

IEC TS 62997

Edition 1.0 2017-06

TECHNICAL SPECIFICATION

Industrial electroheating and electromagnetic processing equipment – Evaluation of hazards caused by magnetic nearfields from 1 Hz to 6 MHz

INTERNATIONAL
ELECTROTECHNICAL
COMMISSION

ICS 25.180.10

ISBN 978-2-8322-4449-4

CONTENTS

INTERNATIONAL ELECTROTECHNICAL COMMISSION

_____

INDUSTRIAL ELECTROHEATING AND ELECTROMAGNETIC PROCESSING EQUIPMENT –

Evaluation of hazards caused by magnetic nearfields from 1 Hz to 6 MHz

FOREWORD

1) The International Electrotechnical Commission (IEC) is a worldwide organization for standardization comprising all national electrotechnical committees (IEC National Committees). The object of IEC is to promote international co-operation on all questions concerning standardization in the electrical and electronic fields. To this end and in addition to other activities, IEC publishes International Standards, Technical Specifications, Technical Reports, Publicly Available Specifications (PAS) and Guides (hereafter referred to as "IEC Publication(s)"). Their preparation is entrusted to technical committees; any IEC National Committee interested in the subject dealt with may participate in this preparatory work. International, governmental and non-governmental organizations liaising with the IEC also participate in this preparation. IEC collaborates closely with the International Organization for Standardization (ISO) in accordance with conditions determined by agreement between the two organizations.
2) The formal decisions or agreements of IEC on technical matters express, as nearly as possible, an international consensus of opinion on the relevant subjects since each technical committee has representation from all interested IEC National Committees.
3) IEC Publications have the form of recommendations for international use and are accepted by IEC National Committees in that sense. While all reasonable efforts are made to ensure that the technical content of IEC Publications is accurate, IEC cannot be held responsible for the way in which they are used or for any misinterpretation by any end user.
4) In order to promote international uniformity, IEC National Committees undertake to apply IEC Publications transparently to the maximum extent possible in their national and regional publications. Any divergence between any IEC Publication and the corresponding national or regional publication shall be clearly indicated in the latter.
5) IEC itself does not provide any attestation of conformity. Independent certification bodies provide conformity assessment services and, in some areas, access to IEC marks of conformity. IEC is not responsible for any services carried out by independent certification bodies.
6) All users should ensure that they have the latest edition of this publication.
7) No liability shall attach to IEC or its directors, employees, servants or agents including individual experts and members of its technical committees and IEC National Committees for any personal injury, property damage or other damage of any nature whatsoever, whether direct or indirect, or for costs (including legal fees) and expenses arising out of the publication, use of, or reliance upon, this IEC Publication or any other IEC Publications.
8) Attention is drawn to the Normative references cited in this publication. Use of the referenced publications is indispensable for the correct application of this publication.
9) Attention is drawn to the possibility that some of the elements of this IEC Publication may be the subject of patent rights. IEC shall not be held responsible for identifying any or all such patent rights.

The main task of IEC technical committees is to prepare International Standards. In exceptional circumstances, a technical committee may propose the publication of a technical specification when

- the required support cannot be obtained for the publication of an International Standard, despite repeated efforts, or
- the subject is still under technical development or where, for any other reason, there is the future but no immediate possibility of an agreement on an International Standard.

Technical specifications are subject to review within three years of publication to decide whether they can be transformed into International Standards.

IEC TS 62997, which is a technical specification, has been prepared by IEC technical committee 27: Industrial electroheating and electromagnetic processing.

The text of this technical specification is based on the following documents:

Enquiry draft	Report on voting
27/1000A/DTS	27/1007/RVDTS

Full information on the voting for the approval of this technical specification can be found in the report on voting indicated in the above table.

This document has been drafted in accordance with the ISO/IEC Directives, Part 2.

In this technical specification, the following print types are used:

- terms used throughout this specification which have been defined in Clause 3: in bold type.

The committee has decided that the contents of this document will remain unchanged until the stability date indicated on the IEC website under "http://webstore.iec.ch" in the data related to the specific document. At this date, the document will be

- reconfirmed,
- withdrawn,
- replaced by a revised edition, or
- amended.

A bilingual version of this publication may be issued at a later date.

IMPORTANT – The 'colour inside' logo on the cover page of this publication indicates that it contains colours which are considered to be useful for the correct understanding of its contents. Users should therefore print this document using a colour printer.

INTRODUCTION

An external alternating magnetic flux can induce electric fields inside the human body. Such induced fields constitute an important category of possible hazards. This technical specification deals with the sub-category of non-radiating magnetic nearfields in the frequency range between 1 Hz and 6 MHz being the source of the induced electric fields. The primary focus is on technical applications in industrial electroheating and electromagnetic processing installations and equipment, with the applicable safety standards in the IEC 60519 series.

IEC 62110:2009 deals with measurement procedures applicable to the characterisation of magnetic and electric field levels with regard to public exposure. IEC 62822-2:2016 provides assessments of exposure restrictions for electric arc welding equipment from 0 Hz to 300 GHz. There is, however, no other IEC standard or technical specification covering more general kinds of equipment and hazard assessments in the range of up to 6 MHz.

Magnetic field hazards are dependent on the source characteristics, including such without and with magnetic materials in the source circuit or workload. Such materials enhancing the magnetic flux density are required for creating an induced electric shock hazard below some few kHz. Static magnetic fields can cause other hazards than those by conventionally induced electric fields and are dealt with in IEC 60519-1:2015. The lower frequency limit in this technical specification is therefore 1 Hz.

NOTE A parallel IEC technical specification IEC TS 62996[1] is developed by IEC TC 27, to cover touch and contact currents and voltages in the frequency range 1 kHz to 6 MHz. It also includes measurements of capacitively coupled currents through the body. Touch and contact currents and voltages at lower frequencies are covered by IEC 61140:2016.

The upper frequency limit 6 MHz is chosen, since

- higher frequencies are not expected to be employed by internal frequency converters for DC voltage transformation in equipment;
- the free space wavelength of 6 MHz is 50 m, which results in wave phenomena that essentially do not exist in or at parts of the human body which have less than 10 % characteristic dimensions of this;
- the power penetration depth limitation by the equivalent complex permittivity of body tissues has not yet set in at 6 MHz, so the magnetic flux completely penetrates the parts of the body under study with no shielding effects, resulting in an overall simpler and linear frequency dependence of the induced electric fields;
- the equivalent complex permittivity of the parts of the body under study is typically so high in this frequency range that external electric fields are efficiently hindered from entering the part of the body and causing internal electric fields – as a consequence, the separation of capacitively coupled and induced electric fields is therefore strong;
- processing frequencies below 6 MHz are typically low impedance; higher impedance dielectric heating has its lowest ISM frequency at 6,8 MHz, being dealt with in IEC 60519-9:2005.

Electromagnetic exposure is commonly defined to occur whenever and wherever a person is subjected to electric, magnetic or electromagnetic fields, and the allowed acceptable levels of exposure are usually specified by national radiation protection or worker protection agencies in the framework of health and safety regulations addressing the user of equipment. Since different sources of information on the associated safety requirements exist and these sources tend to apply quite different safety margins, there are unfortunately significant discrepancies among their levels of the in principle pathophysiologically based so-called basic restrictions.

[1] Under preparation. Stage at the time of publication: IEC/CDTS 62996:2016.

When the source is well defined and is the basis for calculations and computations, the technical treatment of emission is preferred to the consideration of exposure. That is the case in this technical specification, also since the external magnetic nearfield is not modified by the presence of the part of the body nearby. Furthermore, the resulting induced and potentially hazardous internal electric fields depend on the size, shape and orientation of the part of the body in relation to the source, and on the spatial characteristics of the field. Since the induced electric field by magnetic nearfields is directed essentially parallel to the bodypart surface, whereas it is perpendicular for contact current fields, the hazard criteria applied in this technical specification differ from those in some standards.

This technical specification provides complete information for assessments.

The treatment of magnetic nearfields as defined in this technical specification deals with discontinuous presence of the operator in the nearfield, as well as intermittent operation. Cases which do result in shorter term higher body tissue temperature rise in very small tissue volumes are also dealt with in this technical specification. The information and requirements are thus useful for other similar cases in science and industry.

As to measurement procedures and equipment, IEC 60519-1:2015 provides an overview. IEC TC 106 has published standards which provide guidance for situations where the source of the magnetic field and the exposed person are typically further apart than in the situations addressed in this technical specification. As a consequence, those standards tend to define magnetic field sensors neither well suited for measurements very close to current-carrying conductors nor on magnetic fields which vary considerably over the region where the nearest part of the body being submitted to the emission is located.

IEC 62822-2:2016 developed by IEC TC 26 deals with the reduction of the coupling from magnetic nearfields compared with homogeneous fields, as does this technical specification, but in somewhat different ways.

Hazard estimations related to magnetic nearfields pose problems with the use of some existing exposure standards, either by an exaggerated safety margin of the so-called reference levels, or by complicated and expensive numerical modelling in applying the so-called basic restrictions. The methods in this technical specification reduce costs to industry by being simple and direct. They are also realistic, in particular since the number of reported accidents or incidents caused by magnetic nearfields as addressed in this technical specification are exceptionally few in relation to the occurrence of strong such fields in industry.

This technical specification specifies a volunteer test method for assessments of perception of immediate muscle and nerve reactions in fingers and hands at frequencies below 100 kHz. A first argument is that the test ends at the perception level when the person's finger or hand slowly approaches the current-carrying conductor without contacting it, and a distance is measured. There is no risk of harm, unlike with medical tests using volunteers, which require ethical permits, etc. A second argument is that the computational alternative in cases with intricate conductor geometries and possible magnetic materials in the source circuit or workload is highly complicated and therefore expensive, requiring numerical modelling since measurements of the magnetic nearfield is virtually impossible and the induced electric field depends on the positioning of the finger or hand. A third argument is that realistic data are immediately obtained and typically result in the safety distance in most cases being very short and therefore easy to control.

INDUSTRIAL ELECTROHEATING AND ELECTROMAGNETIC PROCESSING EQUIPMENT –

Evaluation of hazards caused by magnetic nearfields from 1 Hz to 6 MHz

1 Scope

This IEC technical specification specifies the characteristics of external magnetic nearfields, computations of and requirements on induced electric fields in body tissues in the frequency range from 1 Hz to 6 MHz with respect to induced electric shock phenomena, for electroheating (EH) based treatment technologies and for electromagnetic processing of materials (EPM). The phenomena include specific absorption rates with time integration.

NOTE The overall safety requirements for the various types of equipment and installations for electroheating or electromagnetic processing in general result from the joint application of the General Requirements specified in IEC 60519-1:2015 and Particular Requirements covering specific types of installations or equipment. This technical specification complements the General Requirements and applies to internal frequency converters for creating high or low DC voltages, and to processing frequencies.

Induced electric shock phenomena dealt with in this technical specification are caused by the alternating magnetic nearfield external to a current-carrying conductor or permeable object, inducing an electric field in a part of the body in the vicinity of the conductor.

Relaxed criteria compared with the general **basic restrictions** for exposure apply. Simplified hazard assessment procedures apply for situations when only fingers, hands and/or extremities are in the magnetic nearfield.

This technical specification does not apply to equipment within the scope of IEC 60519-9. i.e. equipment or installations for high frequency dielectric heating.

2 Normative references

The following documents are referred to in the text in such a way that some or all of their content constitutes requirements of this document. For dated references, only the edition cited applies. For undated references, the latest edition of the referenced document (including any amendments) applies.

IEC 60417, *Graphical symbols for use on equipment* (available at http://www.graphical-symbols.info/equipment)

IEC 60519-1:2015, *Safety in installations for electroheating and electromagnetic processing – Part 1: General requirements*

3 Terms, definitions, symbols and abbreviated terms

3.1 Terms and definitions

For the purposes of this document, the terms and definitions given in IEC 60519-1:2015 and the following apply.

ISO and IEC maintain terminological databases for use in standardization at the following addresses:

- IEC Electropedia: available at http://www.electropedia.org/;
- ISO Online browsing platform: available at http://www.iso.org/obp.

NOTE 1 General definitions are given in IEC 60050, the International Electrotechnical Vocabulary. Terms relating to industrial electroheating are defined in IEC 60050-841.

NOTE 2 Some of the definitions in this clause differ somewhat to those in standards and guidelines, as well as between these. Definitions in this Technical Specification are bolded in the text and several of them have explanatory notes in this clause.

3.1.1
aversion
experience that is disliked but can be accepted for a short time before voluntary withdrawal

Note 1 to entry: Reactions to aversive stimuli are consciously controlled, as opposed to reactions to pain which causes harm and can normally not be controlled.

Note 2 to entry: Typical quotients of internal electric fields between **aversion** and perception in the Hz to kHz range is about 2; see IEC TS 62996:– covering touch and contact currents and voltages in the frequency range from 1 kHz to 6 MHz.

3.1.2
basic restrictions
BR
restrictions on *in situ* (i.e. internal) electric fields or specific absorption rates (**SAR**) or power densities with time and spatial averaging or integration, resulting from a part of or the whole body being subjected to an external alternating electric (E) field, magnetic (B) flux or electromagnetic field, and that are intended to be based directly on resulting established pathophysiological effects

Note 1 to entry: The term exposure is avoided since it has many, even contradictory, meanings. As a consequence, the defined term is not generally applicable outside the scope of this technical specification; see Note 3 to entry.

Note 2 to entry: **Basic restrictions** have a safety margin to harm.

Note 3 to entry: Sources of scientific and medical information on numerical values are e.g. IEEE, ICNIRP and EU. Another term for the limits is exposure limit values (ELV). Levels are different among sources; reasons within the scope of this technical specification are differences in safety factor levels, different considerations of magnetic flux curvatures and decay rates with distance from the source, body surface versus in-depth fields, **coupling values**, and measurement sensors.

Note 4 to entry: Since *in situ* electric field strength or power densities in tissues are secondary to the emitted magnetic nearfield, definitions by IEC TC 34 and TC 106 are not used in this technical specification.

Note 5 to entry: Time factors of **specific absorption rates** (**SAR**) or power densities, i.e. energy absorption versus time, are necessary for establishing criteria.

3.1.3
conductor geometry and current restrictions
CGCR
restrictions on certain combinations of conductor geometry, current, operating frequency (i.e. source properties) and distance/orientation of fingers, hands and extremities in relation to a source with no permeable material being affected, intended to be indirectly based on resulting pathophysiological effects

Note 1 to entry: **CGCR**s for complicated source properties are not considered in this technical specification.

3.1.4
coupling value
relationship between induced electric field strength maximum in a bodypart, the frequency and the inducing magnetic flux density in defined locations, under the assumption that there is no counter-induced magnetic field in the bodypart due to its resistivity

Note 1 to entry: The connection between these is $E = C \cdot f \cdot B$, where E is the electric field strength, C the coupling value, f the frequency and B the magnetic flux density. C is thus in metre.

Note 2 to entry: Examples of the defined location of the B vector flux are near the location of the maximum induced electric field strength or the centre of an induction coil.

3.1.5
electromagnetic emission
phenomenon by which electromagnetic energy is available near a source

Note 1 to entry: For industrial microwave equipment dealt with in IEC 60519-6:2011, emission rather than exposure is also applied.

Note 2 to entry: The source data used in this standard are typically expressed by conductor geometry, current and frequency in cases with no permeable or disturbing material, since magnetic nearfield flux properties are in many cases difficult or even practically impossible to measure with sufficient accuracy.

Note 3 to entry: The energy can be reactive, i.e. non-radiating (evanescent) into free space.

[SOURCE: IEC 60050-161:1990, 161-01-08, modified – The definition has been modified by replacing the words "emanates from" by "is available near" and notes to entry have been added.]

3.1.6
induced electric shock
pathophysiological effect resulting from an internal induced electric field caused by an alternating magnetic flux external to a current-carrying conductor or other flux source

Note 1 to entry: The effects in the frequency range below 100 kHz are essentially immediate, as muscle and nerve reactions. In the higher frequency range these have vanished and time-dependent local overheating constitutes the possible hazard.

Note 2 to entry: With magnetic nearfields the bodypart where the highest electric field intensity occurs is typically that nearest to a current source or the magnetic flux maximum, or a region in which the induced closed current path has a reduced cross section.

Note 3 to entry: No contact currents are supposed to be created, as with conventional electric shock dealt with in IEC TS 62996:–.

3.1.7
magnetic nearfield
magnetoquasistatic field
non-radiating alternating magnetic field existing near a current source, characterised by a field curvature and spatial decay rate at the point of investigation

Note 1 to entry: Typically, these particular influences by **magnetic nearfields** have disappeared at source distances twice the characteristic size of the bodypart.

Note 2 to entry: The field curvature is the radius R_{osc} of the osculating circle.

Note 3 to entry: Comparative calculations or computations of the **coupling value** in a homogeneous magnetic flux are valuable for approximate verifications, but such flux is not a nearfield. There are then cases where calculations and/or magnetic flux measurements are preferred.

3.1.8
pain
unpleasant experience such that it is not readily accepted a second time by the subject submitted to it

EXAMPLE A capacitor discharge corresponding to approximately 1 µF capacitance at 100 V between gripping hands, 3,5 mA AC touch current, the sting of a bee, the burn of a cigarette.

Note 1 to entry: Agents at the pain level cause harm as defined in e.g. IEC 60050-903:2013, 903-01-01.

Note 2 to entry: The examples are objective statements for standardisation purposes. Subjective experiences vary.

[SOURCE: IEC TS 60479-2:–, 3.13, modified – Note 1 has been updated and an example and Note 2 have been added.]

3.1.9
point of investigation
POI
location in space at which the vector value and field curvature, as well as the amplitude spatial decay rate along the radius vector from the source of the magnetic flux, are evaluated

Note 1 to entry: Since decay rates are spatial derivatives, measurements require spatial integration or known properties of the **emission** source. Furthermore, the magnetic field curvature measurement requires more than one **POI**.

Note 2 to entry: There are principle uncertainties regarding the choice of the **POI** in cases with rapidly spatially decaying magnetic flux intensity inside the bodypart. In this technical specification, magnetic flux data are typically given at the surface of the bodypart where the maximum induced electric field occurs. However, the magnetic flux intensity value in a characteristic point such as the centre of a coil is chosen when emission characteristics are used.

Note 3 to entry: The **POI** location and its extent are defined in cartesian, cylindrical or spherical co-ordinates relative to a suitable reference point on the equipment under test.

Note 4 to entry: The field properties at the **POI** are in many cases difficult or even practically impossible to measure. **Emission** characteristics are then instead used; see Note 2 to entry, and 3.1.5.

3.1.10
reference levels
RL
directly measurable quantities, derived from basic restrictions and provided for practical exposure assessment purposes

Note 1 to entry: The meaning of the term differs between some standards and guidelines, with regard to the considerations of safety factors.

Note 2 to entry: **Reference levels** are as such not referring to any levels of immediate nerve and muscle reactions, or sensations of any gradual heating of the tissue.

Note 3 to entry: Another term, by IEEE and EU, is action level (AL).

Note 4 to entry: Considerations of the magnetic flux curvature parameter and amplitude decay with distance from the source are generally not openly described in standards and guidelines.

3.1.11
specific absorption rate
SAR
power absorbed by (dissipated in) an incremental mass contained in a volume element of biological tissue when subjected to an external alternating electric field, magnetic flux or electromagnetic field

Note 1 to entry: The electromagnetic power density is related to only the electromagnetic volume properties of biological tissue, so a recalculation from that to **SAR** has to be carried out using the specific density, which is usually set to 1 000 $kg \cdot m^{-3}$. There is additionally a need for knowledge on the specific heat capacity and heat conductivity of the tissue, as well as power deposition patterns and *in situ* heat conduction or convection properties, for determination of any hazardous temperature rises or rise rates.

[SOURCE: IEC 62479:2010, 3.14, modified – The exposure concept has been generalised and a note has been added.]

3.2 Quantities and units

Apart from the internationally accepted SI units, the following physical quantities are used throughout this document.

Physical quantity	Symbol	Unit	Meaning
Coupling factor	C	m	Defined in 3.1.4; general term.
Coil coupling factor	C_{coil}	m	C, using the magnetic flux in the centre of a single turn coil as reference.
—	$C_{standard}$	m	C, calculated from the basic restrictions and reference values specified in other standards.
Film thickness	d	m	Thickness of an absorbing film with film resistance R_f.
Bodypart thickness	D	m	Characteristic diameter of a bodypart under investigations for induced electric fields.
Penetration depth	d_p	m	The distance from the surface to the layer below the surface of an a halfspace of an absorbing material at which the power density is 1/e of that at the surface, when illuminated by a perpendicularly impinging plane wave.
Relative permittivity	ε	1	The relative complex dielectric permittivity in relation to the electric constant ε_0.
Relative real permittivity	ε'	1	The real part of ε.
Dielectric loss factor	ε''	1	The imaginary part ε. $\varepsilon = \varepsilon' - j\varepsilon''$, where j is the imaginary unit (the positive square root of –1).
Effective permittivity	ε_{eff}	1	The absolute value of ε.
Power density	p	Wm^{-3}	—
Object radius	R	m	Radius of a sphere or long circular cylinder
Distance in air	ρ	m	Distance from the axis of a long straight current-carrying wire to the nearest facing surface of a bodypart
Film resistance	R_f	Ωsq^{-1}	The resistance in ohm per square of a flat absorbing film which is much thinner than the d_p of the material as such.

4 Organisation and use of the technical specification

It is recommended that this technical specification is studied in the listed order below. The order of use then depends on what is deemed to be critical. The annexes provide much data.

a) Firstly, the definition of **magnetic nearfield** in 3.1.7 is important. If such fields and bodyparts fulfil this, the induced electric *in situ* field typically becomes weaker than with a homogeneous magnetic field and is typically concentrated to the peripheral regions of the bodypart.

b) Secondly, Formula (1) in Clause 5 is of central importance. The **coupling value** C is frequency independent up to the highest frequency of 6 MHz dealt with in this technical specification.

c) Thirdly, Formula (2) in 6.2 expresses the basic condition for acceptance of the combination of conductor geometry, bodypart shape and location, and frequency between 1 kHz and 100 kHz. The value at 1 kHz (3,6 Vm^{-1}) applies down to 1 Hz.

d) Clause 6 is applicable for frequencies up to 100 kHz and concerns nerve and muscle reactions which are immediate if the *in situ* electric field strength is high enough. However, with Formula (2) fulfilled there should be no perception. Since there are considerable difficulties to obtain the in situ electric field, indirect methods have to be applied. They are listed in Clause 6, with data handling in Clause 8.

e) Clause 7 deals with requirements related to bodypart tissue overheating. For frequencies above 100 kHz this can occur without any immediate perception. The **specific absorption rate** (**SAR**) concept is used, with relaxations for short-time fast tissue heating which is sensed. Again, computing or calculating the *in situ* electric field strength is necessary. Some methods in Clause 6 are used, with tissue data from Annex C.

f) Clause 8 deals with the overall calculations and safety considerations. In particular 8.6 is important and deals with the different approaches towards compliance. There is a special IEC warning marking for **magnetic nearfields**, reproduced in Clause 9.

g) Among the eight Annexes the first three (A, B and C) are of reference character. Annex D deals with the non-nearfield case of object coupling to a homogeneous magnetic flux, and its Figure D.3 is very illustrative. Annexes E and F deal with objects near a straight wire and coil, respectively, and many results are summarised in Clause F.10 and in the practically useful graphs and tables in Annex G. Finally, Annex H deals with some computational issues and necessities for frequency upscaling in numerical FDTD modelling.

5 The basic relationship for determination of the in situ induced electric field

The most basic and valid relationship between an inducing sinusoidal magnetic flux intensity B in a small closed and homogeneous region where the induced electric field strength E is highest is expressed as

$$E = C \cdot f \cdot B \tag{1}$$

in the SI system, where C is the coupling value in metre and f the frequency in Hz. It follows from the definition of the coupling value C that it is applicable if the magnetic flux is not affected by the presence of the object, i.e. if the object is non-magnetic and has an electric conductivity σ which is sufficiently low for the E field not to be affected by it. Furthermore, humans are considered entirely non-magnetic so the *in situ* $B = \mu_0 H$. It is also to be noted that C is in principle frequency independent since the magnetic field is not influenced by the presence of the bodypart; see Annex H on the limitations.

The general form of Formula (1) is directly applicable with homogeneous B flux and solvable by analytical functions for some mathematically cylindrical geometries with axis parallel to the B field direction. For inhomogeneous B fields there is a need to, in some way, define their structure. Two ways are used in this technical specification:

- for an infinitely long conductor, its cross section dimensions and either the total current in it or the measured/computed B field at the object surface where the maximal *in situ* E field is induced;
- for a single turn coil, all its dimensions and either the total conductor current or the B flux intensity at its centre; the resulting **coupling value** C is then labelled C_{coil}.

NOTE Further basic information, on e.g. 2D modelling, is given in Clause D.1. A differently defined coupling factor K_{2D} and comprehensive 2D modelling results are in IEC 62226-2-1:2004.

The C value depends on the object geometry and location, and on the B flux characteristics. Since the induced E field "strives" to become circular in a homogeneous B flux in a homogeneous conductive body (by the Kirchhoff principle of minimum Joulean heat), it will typically have a minimum in the central regions of an object. There will also be a lower C value for objects which are linearly shrunk in the plane perpendicular to the B flux direction under otherwise unchanged conditions; see D.2.3.

With inhomogeneous tissue conductivity, much the same as above applies, but concentration effects of the current density occur; see Clause F.4. More accurate bodypart models for numerical modelling shall then be considered. However, **magnetic nearfields** typically allow the simplifications made in Annex C.

6 Requirements related to immediate nerve and muscle reactions

6.1 General

Clause 6 specifies requirements on and rationales for applicable maximal in situ electrical fields where **SAR** limitations are not primary, from 1 Hz to 100 kHz.

The particular requirements in this technical specification apply with **magnetic nearfields** in cases where the affected bodypart is only fingers, hands or extremities, as follows:

a) using the **CGCR** method in 6.2; this is applicable in geometrically simple configurations where only the current-carrying conductor and the bodypart are present. Formula (2) in 6.2 is applicable.

b) using numerical modelling, with the **coupling value** C being obtained and used with Formula (1) in Clause 5 and Formula (2) in 6.2. The examples in Annexes C, D, E, F and G provide information which is applicable in cases where the scenario under study is similar.

c) using the volunteer test method in 6.3. This is applicable in cases with complicated geometries and locations and bodypart postures. The method is also applicable in cases where the source circuit contains magnetic materials or a workload is influencing the **magnetic nearfield**.

The **BR** values referred to in Figure A.1 are applicable for other bodyparts than fingers, hands and extremities. However, if it is shown by numerical modelling that the *magnetic nearfield* in combination with the kind and posture of the trunk provides the most onerous induced E field only in shallow regions by a **magnetic nearfield** source close to it, a relaxation down to the specification in Formula (2) is possible to apply.

NOTE 1 Reasons for the modified requirements by Formula (2) in relation to the **BR** values in Figure A.1 are given in Clause A.1.

NOTE 2 It is well known that the immediate nerve and muscle reactions are very much reduced at 100 kHz and still more at higher frequencies, as compared with those at AC mains frequency. For kHz frequencies only a tingling sensation is perceived if the electric field intensity is high enough. The upper frequency limits by ICNIRP/EU and IEEE for immediate nerve and muscle reactions on *in situ* electric fields therefore seem to be unclear with regard to such reactions; there cannot be any pain by such reactions only, at frequencies higher than 100 kHz. If the time of being subjected is short and at a high internal electric field level and high frequency, there are of course difficulties to separate out the direct electrical and tissue heating effects by volunteer studies.

NOTE 3 The immediate nerve and muscle reactions are proportional to the peak value of the *in situ* induced electric field strength, with the time between peaks characterising the frequency f. It is then to be noted that the electric field curveform is related to the time derivative of the inducing magnetic field.

6.2 Method using the conductor geometry and current restriction (CGCR)

NOTE 1 Annexes D to G provide the basis for the restrictions set out in 6.2. In particular, the bodypart models in Annex C and the reported volunteer study results at 11 kHz in Clause F.8 are applied and provide a background to Formula (2).

Using **CGCR** levels with a number of scenarios for obtaining relevant safety levels by numerical modelling shall, alternatively to 6.3, be the conclusive procedure.

The requirement for acceptance in Formula (2) is valid between 1 kHz and 100 kHz for the maximal induced electric field strength in fingers, hands and extremities by a sinusoidal **magnetic nearfield**.

$$E_{\mathrm{RMS}} \leq 3{,}6 \times 10^{-3} \cdot f \quad (f > 1\ \mathrm{kHz}) \tag{2}$$

where E is in Vm^{-1} and f in Hz.

From 1 Hz to 1 kHz the fixed value 3,6 Vm^{-1} at 1 kHz given by Formula (2) applies.

The **CGCR** method is applicable for only sinusoidal magnetic fields with magnetic objects in the circuit. If magnetic fields have an influence, numerical modelling is needed unless B flux measurements in 8.3 or the volunteer test method in 6.3 are carried out.

NOTE 2 Reasons for the higher value than 0,77 Vm^{-1} (EU) and 2,1 Vm^{-1} (IEEE) at 1 Hz are the limitations to these extremities, limits to nearfields, and exclusion of magnetic materials.

NOTE 3 It is in practice not possible to get these E field strength values at frequencies less than 1 kHz unless magnetic materials are used in particular ways for creating the necessary high magnetic flux densities.

NOTE 4 Comparisons between volunteer test results of touch currents at 11 kHz and numerical modelling results with a coil with 4,8 kA at the same frequency are used as a basis. They are described in Clauses F.7 and F.8, with conclusions in Clause F.9. The E_{RMS} value used as reference for **CGCR** calculations is set to 40 Vm^{-1} at 11 kHz sinusoidal fields and is proportional to the frequency.

In this technical specification the outermost skin region with about 2 mm thickness is excluded in the determination of the region over which the spatial averaging of the induced electric field is made. The tissue region to be considered is contiguous, with 4 mm^2 to 6 mm^2 cross section with no concave periphery and at least 1 mm in minimum width, perpendicular to the current flow (and E field direction) and selected as having the highest average.

NOTE 5 Reasons for the skin region exclusion are primarily due to essential shorting-out by the much higher conductivity of inner tissues; see Clause 5, C.2.2 and C.2.3.

NOTE 6 The spatial averaging is in consideration of the possibility of use of various numerical methods, and for avoiding unnecessarily detailed computations. The shape of the cross section is thus elliptical or rectangular.

If the actual scenario is represented in Annexes E to G or numerically modelled, no additional safety factor on the **coupling value** C is applied. In other cases the safety factor of C is set to a number between 1,5 and 2 depending on the similarities. In addition, a safety factor for the reference scenarios shall be applied and specified in the documentation, in consideration of all geometric factors including positions of the operator finger, hand or extremity as well as conductor geometry, current and frequency.

6.3 Volunteer test method

6.3.1 Volunteer basic test method

The primary use of this method is with conductor, workload conditions including presence of permeable materials and bodypart locations and orientations for which the **CGCR** method is not deemed suitable and the similarities to the reference scenarios in annexes are insufficient, or numerical modelling facilities are not available. In particular, the method is suitable when there are permeable materials affecting the magnetic flux inducing electric fields in bodyparts.

The goal is to ascertain that the scenario – i.e. all geometric factors including the operator finger, hand or extremity in an onerous but not unlikely position and posture, as well as source type, geometry, current and frequency – will not result in an immediate nerve or muscle reaction. The method is applicable for frequencies up to 100 kHz, for non-sinusoidal and sinusoidal induced electric fields.

NOTE 1 For frequencies lower than some few kHz, sufficient inducing magnetic flux densities are possible to achieve only with permeable materials in the source circuit.

NOTE 2 The method is not applicable for frequencies and conditions which result in tissue overheating being the primary hazard.

If maximally one of four volunteers perceives nerve reactions and none of the four experiences aversion with the highest normal operating current, the scenario is compliant.

Other criteria of volunteer selection and test results can be required by national authorities for worker protection.

NOTE 3 The method with elevated currents or closer approach to the conductor in 6.3.3 is preferred, if technically possible.

NOTE 4 An example in given in Clause F.7.

6.3.2 Method based on volunteer tests and similarity with pre-existing scenario

This is applicable in cases of changes of coil radius or conductor length, workload if existing, and change of frequency, all with unchanged access by the relevant bodypart. No further assessments are then needed for compliance.

NOTE Annex B provides formulae for recalculations, or numerical modelling can be carried out instead.

6.3.3 Method based on volunteer tests, using available elevated conductor current or shorter distance between the conductor and bodypart

Elevated currents improve the assessments of the level of perception. If with an otherwise unchanged scenario maximally one of the four volunteers as in 6.3.1 express **aversion**, the relative elevated current becomes a safety factor to be applied with e.g. characteristic size of the bodypart or the distance to the source.

NOTE 1 Shorter distances between the conductor and bodypart is an applicable method as above, for reasonably straight conductors but not with coils. There are in some cases variations of the C value with distance; see Table E.1 and Figure G.1.

NOTE 2 Annexes E and F provide relevant information.

6.3.4 Method using magnetic nearfield reference levels (RLs)

This is applicable in cases where the magnetic flux is measurable close to the **POI**, which shall be at least 20 mm from the nearest point on the magnetic flux source. The applicable RL B value is $1{,}0/f$ T (RMS) from 1 Hz to 6 MHz, with a ceiling value of 300 µT. This applies to all bodyparts for sinusoidal fields.

NOTE 1 Using Formula (1), this corresponds to C = 1 m. That is higher than can realistically be obtained; see Annexes C to G.

NOTE 2 The RL values corresponds well to those in Directive 2013/35/EU. RL values in the IEEE standards are much lower for the lowest frequencies, but has a more than three times higher ceiling value for extremities.

NOTE 3 For non-sinusoidal fields, see 6.1, Note 3.

7 Requirements related to body tissue overheating

7.1 General

7.1.1 The limits of the ICNIRP/EU and IEEE BRs shown in Figure A.1 are specified by these for only averaging over any 6 minutes, and are essentially the same in this Technical Specification, by a slightly modified requirement in 7.1.2. Short term or intermittent bodypart heating requirements are given in 7.2 and 7.3, with temperature rise requirements in 7.1.3 and 7.1.4. Skin heat capacity data are given in 7.3.2, but maximal energy density requirements are specified.

The effective (RMS) value of the *in situ* induced electric field strength is applicable. The electric field curveform is related to the time derivative of the inducing magnetic field.

As for the immediate nerve and muscle reactions, the **CGCR** method and numerical modelling are used for the conditions of possible continuous presence by the bodypart in the **magnetic nearfield**. Requirements are in 7.1.2 to 7.1.4. Cases where this is not practical or possible, and where the magnetic fields are supposed to be so weak that there can be no hazards, are dealt with in 8.6. Intermittent heating is dealt with in 7.2. Short time heating and integration times requirements are specified by volunteer sensing, in 7.3.

NOTE 1 The upper frequency limits of the ICNIRP/EU and IEEE BRs shown in Figure A.1 are at 10 MHz and 6 MHz, respectively. However and as also shown in the figure, limitations by body tissue SAR averaged over any 6 minutes set in at electric field levels many times lower than at the upper frequency limits for the immediate nerve and muscle reactions.

NOTE 2 In view of the recommendations on elevated **SAR** values in Clause 7, there is an uncertainty as to which criteria – E field or **SAR** – should be used before safety factors are applied in cases in the MHz range. The situation is exacerbated by the lack of ICNIRP/EU and IEEE explanations of the chosen frequency proportionality factor f with the simple exponent 1 for the immediate nerve/muscle effect. The ICNIRP safety factors are also stated to be high and can explain the differences to IEEE standards, rather than do any differences among volunteer studies.

7.1.2 The ICNIRP or IEEE BR specifications, or those by the relevant national authority, shall be used for assessing the overheating of a part of the body possibly lasting over any 6 minutes.

Unless particular circumstances motivate otherwise, body average data in Figure C.1 are used.

NOTE 1 A power density of 20 Wkg^{-1} over 6 minutes corresponds to an approximate energy of 7,2 $kJkg^{-1}$ and causes a temperature rise of about or less than 3 K in typical body tissues under conditions of no heat losses to ambient or other bodyparts.

NOTE 2 It is assumed that a continuous heating rate fulfilling the **BR SAR** requirement is not perceived by the person.

7.1.3 It is assumed that the temperature rise in any parts of the body does not exceed 5 K, except for heated skin regions (epidermis/dermis/subcutis) where the local short term temperature is allowed to become 50 °C.

7.1.4 It is assumed that the initial temperature of the skin and fingers is 32 °C, on which the assessments for some intermittent conditions are based. An initial temperature of 40 °C is assumed for other parts of the body, and shall also be used for the initial skin temperature in all situations with elevated ambient temperatures.

NOTE 1 The finger skin temperature rise is thus maximally 18 K for an initial temperature 32 °C, and 10 K for other parts of the body and for finger skin under conditions of elevated ambient temperature.

NOTE 2 Skin data and skin heat capacity considerations, as well as compatible temperature rise criteria for touch currents, are in IEC TS 62996:–, 9.3, 9.4 and Annex C. Compatible electromagnetic finger skin volume data are given in Annex C in this Technical Specification.

7.2 Intermittent conditions with 6 minutes time integration

7.2.1 Subclause 7.2 is applicable for cases where the immediate heating effect extends 6 mm or more into the tissue.

NOTE 1 The determination of this heating depth is to be made by numerical modelling, or by using applicable existing theoretical or numerical data. See Annexes D, E and F.

As a consequence, higher short term **SAR** ceiling values are allowed under the condition that the average over any 6 minutes does not exceed the **BR** value. This ceiling value is set to 500 Wkg^{-1} for fingers, hands and extremities and 250 Wkg^{-1} for other tissue. As a consequence at these ceiling values, the allowed total time of bodypart heating becomes 15 seconds over any 6 minutes.

NOTE 2 The **SAR** factor 500/20 = 25 is compatible with some existing national regulations.

NOTE 3 A discussion of intermittent exposure, with conclusions for microwave industrial equipment, is in Annex BB of IEC 60519-6:2011. The impinging power flux density factor is 5 over maximum 20 seconds duration, but that factor is limited by characteristics of commonly available measurement instruments. The equipment and its control system shall be so designed and set that the resulting energy deposition in any 10 cm^3 fingers, hands and extremities, and that 3,6 MJm^{-3} energy deposition in any 10 cm^3 other tissue is not exceeded over any 6 minutes.

7.2.2 The numerical values in 7.2.1 are allowed also under the condition of non-repetitive operations, with appropriate warning marking and user instructions displayed at the equipment.

7.3 Intermittent conditions in fingers and hands with shorter integration times

7.3.1 Subclause 7.3 is applicable for non-repetitive cases where the immediate heating effect is strongest in a region down to 4 mm or less including the surface of the tissue. Such cases occur in extreme nearfields in the close vicinity to current-carrying conductors.

7.3.2 Skin tissue (2,5 mm total thickness of epidermis, dermis and subcutis) has a heat capacity of about $0{,}62 \cdot J \cdot cm^{-2} \cdot K^{-1}$ per cm^2 area ($6{,}2\ mJ \cdot mm^{-2} \cdot K^{-1}$). Heating by 1 K requires 0,62 J per 0,25 cm^3, i.e. 2,5 J/(cm^3,K). One then typically sets 1 kg tissue approximately equivalent to 1 dm^3.

7.3.3 The tissue volume over which energy deposition integration is made is a 2,5 mm to 3,5 mm thick surface layer.

7.3.4 The power density shall be so high that sensing occurs. The perception conditions for hazard calculations are skin temperature rises of at least 3 K over 5 seconds. The data in 6.3.2 result in a heating by the minimum 3 K requiring 1,5 W/cm^3 = 1,5 MWm^{-3} over the maximum 5 seconds.

7.3.5 The withdrawal reaction in this case is set to be completed 1 second after the actual sensing, i.e. 3 K temperature rise. In the minimum power density case for perception, the temperature rise will thus be about 3,6 K. If the heating rate is higher, maximally 18 K (10 K with elevated ambient temperature) is allowed according to 7.1.3 and 7.1.4. With 15 times higher heating rate than the minimum 1,5 $kJkg^{-1}$, i.e. 22,5 $kJkg^{-1}$, the temperature rise rate becomes 9 Ks^{-1}. This is the maximally allowed local power density.

7.3.6 The temperature evening-out by heat conduction has a time constant of 15 seconds to 20 seconds, with the restriction in 7.3.1. The frequency of repetitive operation resulting in heat perception shall be maximally one per minute.

7.3.7 Appropriate warning marking and instructions shall be displayed at the equipment.

8 Calculations and numerical computations of induced E field and SAR by magnetic nearfields: inaccuracies, uncertainties and safety factors

8.1 Principles for handling levels of safety – general

Achieving an overall acceptable safety requires a combination of a number of often complicated and quite different factors, some being more important than others. Due to their typical interpendencies, summation of the probabilities shall not be linear but basically least-square. Experiences typically show that the dominant uncertainties are related to operator behaviours, including risk awareness, use of information and adherence to instructions. Lack of clear information, instructions and warnings are also important factors. As a consequence, proper instructions by the manufacturer and continued follow-ups by the user are crucial.

The manufacturer has the prerogative to minimise the inherent risks of the equipment by technical means, without disabling the intended process or usability of the equipment. He shall compare the importance and detailed specifications of any such means with the endeavours to minimise the overall risks by proper information and instructions to the user. The balancing of usability and overall safety is a matter of agreement between the manufacturer and the user of the equipment emitting **magnetic nearfields**. It is, however, the responsibility of the manufacturer to pre-assess the competence of the user and his ability and willingness to adhere to all safety instructions by the manufacturer, in consideration of the complexity of the particular EH and EPM installations.

A means for the manufacturer to reduce the inherent equipment risks is to employ various “fool-proof” measures, such as proximity sensors/switches which de-energise the potentially hazardous subsystem of the equipment under conditions of operator errors otherwise

resulting in the operator being subjected to potentially hazardous **magnetic nearfield** emissions. The user shall be specifically informed on such means for interrupted processing, and they shall be specified in the manufacturer's documentation, with their implications.

8.2 The C value variations with B field curvature

As quantified in mainly Table E.1 and Figure G.1, the **coupling value** C to an unchanged part of the body is typically reduced with a small and shrinking curvature radius R_{osc} of the B flux at the **POI**; R_{osc} is the radius of the osculating circle determined by the directions of the B vector of equal amplitude in two nearby locations. If reliable numerical modelling is carried out, this allows relaxations regarding either the allowed approach distance of a part of the body to the **emission** source, or higher currents in it; also see Figure G.2 for an example.

If the field decay rate from the source is strong in relation to the curvature of this part of the body, or strong due to the **emission** source characteristics of e.g. a current loop (see Formula B.4), the *in situ* current path will become limited to only a small region of the part of the body, thus typically getting a much smaller **coupling value** C than in the non-nearfield case. The extent of this weakening of the coupling can in practice be quantified only by numerical modelling, as illustrated in Annexes E, F and G for some typical cases.

8.3 Location of parts of the body, instrumentation and measurement issues

A coil-type sensor is useful in a homogeneous magnetic (B) flux, since the coil area is not important. As addressed in Clause A.2, the region over which the induced E field **BR**s apply is in the order of some few millimetres, and 10 cm^3 or less for the **SAR BR**s. This means that the distance between the bodypart where maximum E is induced and a current-carrying conductor within some decimetres shall be very well known/specified, and/or the B values be measured quite precisely where the bodypart is supposed to be present. For example, 10 mm distance difference at 30 mm average distance from a long current-carrying conductor theoretically results in a B flux quotient of 1,4, i.e. 40 %. This geometric uncertainty factor becomes even higher near coils; see Formula (B.4), and examples in F.2.2.

Another consequence of the location issue is that coil-type B flux sensors have a significant spatial extension, resulting in an averaging of the B flux over the measurement coil area. This average will of course be lower than the maximum closest to the current-carrying conductor.

These issues will in many cases be insurmountable. As a consequence, a procedure of source characterisation and currents (**CGCR**) and an alternative method of volunteer tests are applied in this Technical Specification.

8.4 Handling of inaccuracies of *in situ* E field and SAR numerical values

These quantities cannot be determined by actual measurements, since they have to be non-invasive. As a consequence of the resulting analysis of the overall hazards discussed in 7.1, several of the numerical uncertainty factors in current measurements and geometric as well as tissue property relevancies, numerical modelling of the **emission** and other calculations shall initially be set to low values in the overall risk assessment procedure. This shall be followed by repeated statistical analyses with insertion of the likelihoods of the dominating individual risk levels with modified uncertainties of them, for finding out the few most likely onerous risk factor combinations.

NOTE As an example for users of handheld devices, IEC 62209-2:2010 states that **SAR** overestimates are to be as small as possible and values in the order of 20 % or less are deemed reasonable. It is furthermore stated that tissue conductivities are not to be selected to be arbitrarily large. However, such a statement is applicable by limiting the figure to only the outcome of the numerical modelling as such, for a pre-specified scenario.

8.5 Approaches to compliance

8.5.1 General

It is possible to make assessments based on different methods depending on the accuracy requirements and how close the actual induced E field strength is in relation to the requirement. Separate assessment procedures are applicable also to different parts and operations of the equipment.

NOTE Requirement and risk group classifications are dealt with in Clause 9.

8.5.2 Cases where verification of levels being below the RL is sufficient

NOTE 1 Some **RL** data are given in Annex A.

The **magnetic nearfield** curveform and amplitude in a relevant **POI** in the region of likely or possible bodyparts presence are measured, and the **RL** data in 6.3.4 are found to be significantly higher. No further elaborations are needed if there is a sufficient measurement inaccuracy margin.

NOTE 2 This Technical Specification does not specify C_{standard} levels.

NOTE 3 The accessibility is determined in accordance with 6.3.4 and the relevant specifications and requirements in IEC 60519-1:2015.

8.5.3 Cases where only B flux measurements are sufficient

Measurements are carried out, and it is found that levels exceed or can exceed the **RL** data in an applicable standard or national regulation.

NOTE See Note 2 in the definition of **RL** (3.1.10): the B field curvature parameter for **magnetic nearfields** is not considered in some standards specifying **RL**s, resulting in the **RL** values being too low for such cases.

The field structure of the **emission** is assessed and compared with relevant data in Annexes B, E, F and G. If a reasonable similarity is then found, calculations are made to determine if immediate nerve and muscle reactions or tissue heating is the type of hazard. In the latter case, the duration and frequency or regularity of bodypart presence is used, with the specifications in Clause 7 and Annex B.

Further and final assessments are then made iteratively, after modifications of access or other protection means, if needed.

8.5.4 Cases where the volunteer test method is applicable

This method has the important advantage of being direct in the sense that most computation and calculation errors are inherently eliminated. It is applicable between 1 Hz and 100 kHz for nerve and muscle reactions (see 6.3) and for intermittent conditions in fingers and hands with shorter integration times for higher frequencies (see 7.3).

Detailed records containing information on the individuals, wet/moist conditions, and geometric factors shall be prepared.

The method is applicable in cases where there are clear specifications on minimum distance of the finger, hand or extremity to the current-carrying source, and the source is well-specified. It is particularly suitable when fingers or hands are not straight as specified in Annex C. Gripped tools, if any, are also included in the tests.

8.5.5 Cases where the CGCR method is applicable

This method has the important advantage that magnetic field measurements are typically avoided. As with the method in 8.5.4, detailed geometric factors shall be specified.

The method is particularly applicable in cases where the source frequency and currents vary, and the bodyparts in the nearfield are well defined but their closest distances to the source can vary.

8.5.6 Cases where numerical modelling is carried out

This is applied in situations where there are reasons not to apply any of the methods in 8.5.4 and 8.5.5, for example by the presence of disturbing objects which can alter the magnetic field data, or with complicated source geometries. Current and frequency measurements, including the curveform, are however carried out for scaling purposes. Resources and sufficient knowledge shall be available. Data in Annexes A to G shall be used as basic references for verifications and/or comparisons; other verified references are also allowed.

NOTE If numerical modelling is not accessible and the methods in 8.5.4 or 8.5.5 are not applicable, 8.5.2 or 8.5.3 are applied, with introduction of larger overall safety margins according to Clause 9.

A geometric model of the relevant parts of the equipment is constructed. Then using the measured conductor current(s) or magnetic field(s) in some characteristic locations, the complete scenario is constructed, including tissue conductivities from Annex C. Results are then used, with relevant safety factors.

Frequency upscaling is recommended with finite difference time domain (FDTD) methods. This is addressed in Annex H.

8.6 Summary of inaccuracy/uncertainty factors to be considered

The items dealt with in Clause 8 and to be considered are summarised as follows:

a) Basic issues:
   - The extent of relevance of standardised scenarios (see Annexes D to G) for numerical modelling;
   - Computation inaccuracies and sensitivities (e.g. numerical errors, resolution limits of small spatial distances, non-linearities in frequency upscaled scenarios).

b) Technical and bodypart variabilities:
   - Sensor inaccuracies;
   - B flux measurement uncertainties (manual handling, location of spatial inaccuracies, instrument sensor integration area);
   - Source variabilities (source energising data and frequency, including its spectrum);
   - Variabilities of the relevant parts of the body (tissue electromagnetic properties and geometries, most onerous locations).

c) Operator and user behaviour factors:
   - Time variabilities in operator approaches to and withdrawals from the **emission** source region;
   - Overall influences by operator knowledge and awareness/sensing;
   - Influences by quality of instructions and warnings;
   - Importance of continued information to existing and new staff.

9 Risk group classification and warning marking

9.1 General

Due to the typical lack of personnel experience of possible hazards by **induced electric shock**, and the likelihood of the maximum induced electric fields not occurring in the skin region, risk group settings shall be more severe than for conventional electric shock. A further reason for this is that *in situ* measurements are not possible to carry out.

The safety classification scheme for exposure risks in Table 3 in IEC 60519-1:2015 is applicable as stated in the following 9.2. to 9.6. The application of risk groups 2 and 3 requires special restrictions and hindering of access and are allowed only in such cases where the occurrences of harm are deemed very unlikely after a thorough documentation procedure and instruction work has been carried out and the particular type of equipment and process can reasonably not be used without the very strong magnetic fluxes.

NOTE Risk assessment and categorisation is dealt with in IEC 60519-1:2015. Especially the concepts provided in its Clause 4 are relevant also for **induced electric shock**.

9.2 Induced electric fields from 1 Hz to 1 kHz

The allowed field strength occurs with **magnetic nearfields** only with magnetic materials in the circuit. Due to the associated general calculation and computation difficulties, risk group 0 or 1 applies, with warning signs if group 0 and also instructions if group 1.

9.3 Induced electric fields from 1 kHz to 100 kHz

Risk group 0 applies if the applicable RL value complies with 6.3.4 and 8.5.2.

Risk group 0 still applies if the B field measurements and following calculations in 8.5.3, with an applied safety factor 2 to those given in 6.2 is fulfilled. Without this safety factor, risk group 1 applies.

The same principle as above applies with the volunteer test method: risk group 0 when a safety factor 2 is applied to the **induced electric field**, otherwise risk group 1.

In cases where numerical modelling is carried out, the same principle as above is applied, with risk group settings depending on how well the scenario represents the actual situation. As a consequence, risk group 0 or 1 applies.

9.4 Induced electric fields from 100 kHz to 6 MHz

Risk group 0 applies if 7.1.2 (long term) is fulfilled. Normally, no warning sign is needed.

Risk group 0 also applies with 7.2; a warning sign shall be used.

Risk group 0 or 1 applies with 7.3; measures are specified in 7.3.7.

9.5 Magnetic flux fields from 1 Hz to 6 MHz

Since only **RL** values of such fields are specified in this Technical Specification, risk level 0 applies under the condition that access is hindered at least 20 mm from the nearest part of the source. If not, other methods ensuring safety apply; see 6.2, 6.3 and 8.

9.6 Warning marking

Warning marking shall be according to 19.4 and Annex F of IEC 60519-1:2015.

Symbol IEC 60417-6204:2013-07 “Caution, static magnetic field hazard”, shown on the right in Figure 1, shall be used in cases where the B field source contains magnetic materials and there is a risk of forces on objects. Symbol IEC 60417-6205:2014-08 “Caution, alternating **magnetic nearfield** hazard”, shown on the left in Figure 1, shall be used in cases with strong inducing currents. Both signs shall be used simultaneously, if applicable.

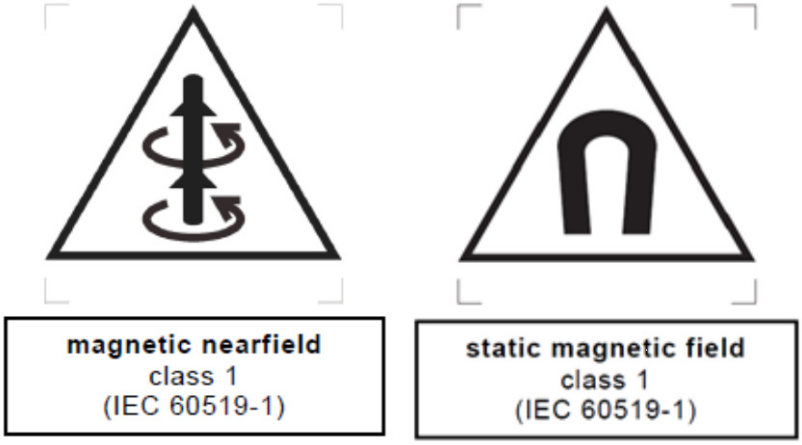

Figure 1 – Examples of warning marking

Annex A
(informative)

Survey of basic restrictions, reference levels in other standards, etc.

NOTE The term basic restrictions in this Annex refers to the definitions of it in the respective standards and guidelines. The term is therefore not bolded.

A.1 Basic restrictions – general and deviations

The main updated original sources on which limits and regulations are based are developed by ICNIRP and by IEEE. IEEE C95.1:2005 uses the *in situ* E field of very short duration as basic unit for hazardous nerve and muscle reactions, whereas ICNIRP changed the underlying physical effect used in their guidelines from *in situ* current density to *in situ* E field, between 1998 and 2010.

The ICNIRP, IEEE and EU BR specifications are outlined in Figure A.1. These, or those by the relevant national authority, constitute reference data for assessing the immediate nerve and muscle reactions as well as tissue heating except in cases dealt with in Clause 6 and short term intermittent conditions in Clause 7.

Formula (2) in 6.2 can be compared with the data illustrated in Figure A.1. As an example, the IEEE C95-1:2005 standard specifies $E_{\mathrm{RMS}} \leq 6{,}27 \times 10^{-4} \cdot f$ which is 5,75 times lower. However, that formula is stated to be valid under all circumstances whereas Formula (2) in 6.2 applies only with the **CGCR** method and numerical modeling. Rationales for Formula (2) are given in Clause F.8 on volunteer studies, and in Clause F.9 by comparisons with conventional electric shock effects by contact current using the impedance data in IEC TS 62996.

Spatial averaging specifications according to ICNIRP, IEEE and EU are given in Clause A.3. They do, however, not consider the particular property of the in situ electric field direction induced by a **magnetic nearfield** to be parallel to the bodypart surface and by that essentially perpendicular to the nerve fibres in the skin region so that no currents are induced in them; see Clauses F.8 and F.9.

NOTE 1 In the Directive 2013/35/EU it is stated that the BR/RL system can be in conflict with specific conditions which should then be taken into account; that employers are entitled where relevant to take exposure levels and other appropriate safety-related data provided by the manufacturer into account; that amendments should be possible taking into account technical progress, changes in the most relevant standards or specifications, and new scientific findings concerning electromagnetic fields. It is furthermore stated in the Directive that evidence for such deviations must then be available.

NOTE 2 In the IEEE standard C95.1:2005 it is stated that its existence does not imply that there are no other ways to produce, test, measure, purchase, market, or provide other goods and services related to its scope. It is also stated that when a document is more than five years old and has not been reaffirmed, it is reasonable to conclude that its contents, although still of some value, do not wholly reflect the present state of the art. The C95.1a Amendment (2010) does not deal with magnetic fields emanating from an alternating current source.

A.2 The coupling values C in ICNIRP guidelines and IEEE standards

With BR and RL data available, C_{standard} values are obtained by insertion of these in Formula (1). The ICNIRP:2010 C_{standard} value for frequencies 3 kHz to 10 MHz is 10 m. IEEE C95.1-2005 has the corresponding C_{standard} value 1,02 m between 2 250 Hz and 5 MHz. Also see Note 2 in 6.3.4.

NOTE 1 Both ICNIRP and IEEE have limited their considerations to cases with a significantly longer distance from the source to the nearest parts of the body than in this Technical Specification. The parts are then also assumed to be so large that very good coupling to the **emission** occurs.

NOTE 2 ICNIRP:1998 discusses a simple first order formula for calculation of the maximum coupling from a homogeneous magnetic field (in its section 4, on **reference levels**) which can be expressed as $C = \pi R$, with R being the radius of the object. Inserting the realistically largest long cylinder approximately representing a head having 200 mm diameter, in a homogeneous B field, in Formula (1) gives C = 0,314 m.

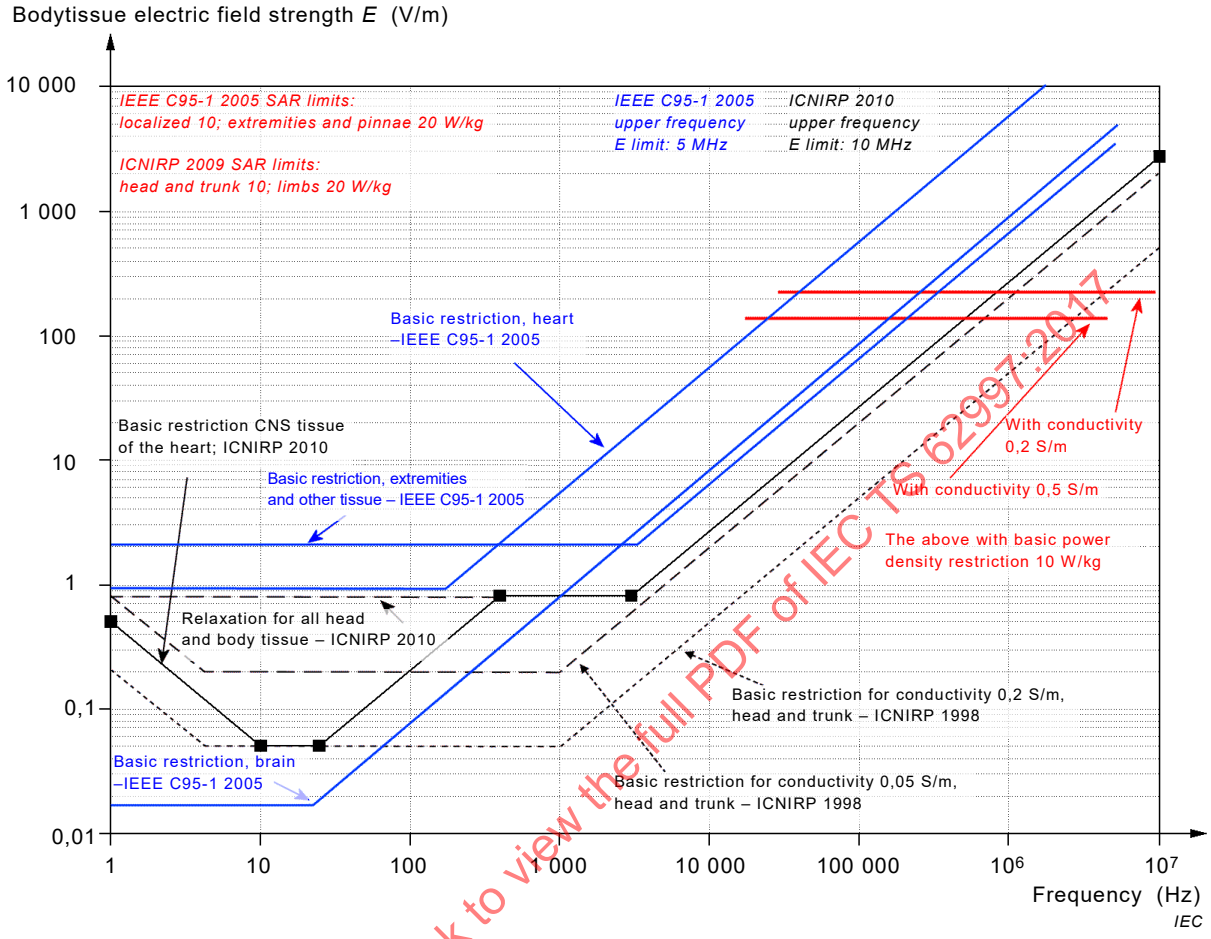

Figure A.1 – ICNIRP, IEEE and 2013/35/EU basic restrictions (RMS)

NOTE 3 Figure A.1 data in red are for thermal effects, dealt with in 7.1. The IEEE, EU and ICNIRP BR values are essentially the same.

NOTE 4 The specifications in 2013/35/EU for induced electric fields is essentially identical to those in ICNIRP 2010 for all head and body, but applies to all tissues. The only difference is that peak value instead of RMS are specified. The values are identical for sinusoidal curveform.

NOTE 5 Since the induced electric field is virtually independent of the electric conductivities of typical human tissues within the frequency range and scope of this Technical Specification, the change by ICNIRP between 2009 and 2010 (from current densities to electric fields) results in an improvement of accuracies or calculated or computed data for comparisons with the E field BR.

NOTE 6 IEEE standards and ICNIRP guidelines deviate considerably between them with regard to the electric field BR, as shown in the graphs in Figure A.1. At 10 kHz, the BR quotient for extremities is about 2 between IEEE and ICNIRP 2010. Between IEEE and ICNIRP 1988 (reconfirmed in 1999) the quotient is about 10, for tissue conductivity 0,2 Sm^{-1}. ICNIRP has not provided any discussion of these differences, except statements that safety factors and worst conditions are considered. IEEE standards include discussion of safety factors, which are stated not to be large but sufficient.

A.3 Basic restrictions – immediate nerve and muscle reactions

According to the ICNIRP guidelines and IEEE standards, *in situ* electric field values shall be spatially integrated over quite small volumes. ICNIRP specifies a small contiguous volume of 2 mm × 2 mm × 2 mm, and IEEE the arithmetic average determined over a straight line segment of 5 mm length oriented in any direction within the tissue. The Directive 2013/35/EU provides no information on spatial integration.

With regard to the immediate nerve and muscle reactions, an agent such as a **magnetic nearfield** at kHz frequencies causes the same kind of perception as does a contact current in the same frequency range, with the only exceptions that:

- in the contact current case there is a tingling sensation in the contacting region as well as in other bodyparts, in principle all the way to the secondary contact area;
- with **magnetic nearfield emission** the tingling effect occurs only in a limited region of tissue where the induced electric field is strongest; this region is in principle quite near the bodypart surface.

There is a generally accepted basic understanding that perception of touch- or contact currents is "not *per se* hazardous but could be considered as annoyance" as stated by e.g. ICNIRP. As a consequence, there is no basic reason to treat the immediate nerve and muscle reactions by touch/contact differently from induced E fields in tissues.

A.4 Basic restrictions – specific absorption rates (SAR)

The main updated sources are the same as in Clause A.2. They are in good agreement and indicated in red in Figure A.1. It is to be observed that the published **SAR** levels are averages over 6 minutes, and that no short time ceiling values are provided. The ICNIRP 1998 and 2010 guidelines, IEEE C95.1:2005 standard and EU Directive 2013/35/EU all specify **SAR** averaging over any 10 g of contiguous tissue.

NOTE 1 Information on the resulting temperature rise is given in 7.1.2, Note 1.

NOTE 2 Modified requirements for industrial microwave equipment, based on bodypart heating rates, etc. are specified in IEC 60519-6.

A.5 Reference levels – external magnetic B field

ICNIRP:2010 specifies B_{max} = 100 µT for all parts of the body, in the frequency interval between 3 kHz and 10 MHz, which is of main interest for this Technical Specification. ICNIRP:2010 states that this applies for conditions where the field variation over the space occupied by the body is relatively small, i.e. non-nearfield cases.

IEEE C95.1:2005 specifies B_{max} = 615 µT for the head and torso and 1 130 µT for the limbs, in the frequency interval 3 350 Hz to 5 MHz. IEEE C95.1:2005 states that if the field is not constant in magnitude or direction over the part of the body, the lower RL applies but it is then permitted to rely on BR compliance.

2013/35/EU specifies B_{max} = 300 µT for "exposure of limbs to a localised magnetic field", and 100 µT for all other all parts of the body, in the frequency interval between 3 kHz and 10 MHz. For frequencies 1 Hz to 3 kHz, B_{max} = 0,9/f T, with f in Hz.

All sources declare that compliance with the basic restrictions is ensured if there is compliance with their RL data, and that lack of compliance with the RL data does not necessarily indicate lack of compliance with their BR data.

In conclusion, the RL specifications differ by a factor six to ten between the IEEE standards and ICNIRP guidelines. This quotient is larger than the one between their BR values in the same frequency interval, which differ by a factor 2,32; see Figure A.1.

Annex B
(normative)

Analytical calculations of magnetically induced internal E field phenomena

B.1 Some basic formulas – magnetic fields and Laws of Nature

Analytical calculations of the magnetic fields at straight conductors and circular coils are straightforward and are obtained from the Biot-Savart law by integration. For a short straight z-directed conductor section, which occurs in e.g. a rectangular loop, the magnetic flux density (B) value outside the centre z = 0 (in cylindrical co-ordinates $\rho\varphi z$) of the conductor with length ± L (i.e. total length 2 L) and carrying a current I becomes

$$B_\varphi = \frac{\mu_0 IL}{2\pi\sqrt{L^2} + \rho^2} \tag{B.1}$$

which for an infinitely long straight conductor simplifies to

$$B_\varphi = \frac{\mu_0 I}{2\pi\rho} \quad (L \to \infty) \tag{B.2}$$

With two parallel conductor sections with parallel or antiparallel current directions, simple vectorial addition or subtraction of the φ-directed field components applies.

The field in an arbitrary point from the centre of a magnetic dipole is again obtained from the Biot-Savart law by integration. It can be shown that the B value at a point z_0 on the z axis (θ = 0; spherical co-ordinates $r\theta\varphi$) of a φ- directed loop with radius b carrying the current I is

$$B_z = \frac{\mu_0 Ib^2}{2\left(z_0^2 + b^2\right)^{3/2}} \quad (\theta = 0) \tag{B.3}$$

At a distance $|R|$ and at the polar angle θ from the centre of the magnetic dipole such as a circular loop with axis in the z (θ = 0) direction and with radius b, and in spherical co-ordinates $r\theta\varphi$, the B value becomes

$$B_r = \frac{\mu_0 Ib^2}{4R^3}\ 2\cos\theta\,;\ B_\theta = \frac{\mu_0 Ib^2}{4R^3}\ \sin\theta \tag{B.4}$$

The induced electric (E) field in an object nearby depends on its geometry and location in relation to the B field, and on the field characteristics of the source. What happens in the theoretical/analytical sense is determined by Faraday's law, linking the vector E and B force fields by the following vector formula:

$$\nabla \times E = -\frac{\partial B}{\partial t} \tag{B.5}$$

In practice, this formula has a simple solution only in special simple cases; see Clause B.2.

In the case of a homogeneous B field such as in the central region of a Helmholtz coil, or at a very long distance from the source, the characteristic E field intensity is highest at the object periphery and zero in the centre region. In cases with small R_{osc} of the B field, the E field intensity is highest in small surface regions; see Annexes E and F.

B.2 Induced field deposition in tissues by magnetic nearfields

In the frequency range within the scope of this Technical Specification, and in consideration of the electromagnetic properties of tissues in this range, there is no significant counter-induced magnetic field by action of the generalised Ampere's law $\nabla \times H = J + \partial D/\partial t$ for the source fields. This is due to the wavelength and penetration depth data as discussed in Annex H.

The induced E field pattern in a homogeneous object with tissue properties is thus independent of the electromagnetic properties, and follows a number of criteria, derivable from Faraday's law in Formula (B.5).

The induced current in the object behaves as if sourceless, since there are no displacement currents outside the object. The Formula of continuity

$$\nabla \cdot J = 0 \tag{B.6}$$

applies, where J is the current density vector. It is an expression of Kirchhoff's current law. The current pattern in the object will thus have a looplike shape with a zero and the overall current around it becoming continuous, but with variable current density. The overall E field pattern will thus to a large extent be determined by the current continuity. In particular, the skin region (see Clause C.2 for data) will partially be shorted out by the higher conductivity of muscle and other interior tissue, due to the current mainly being parallel to the bodypart surface, whereas it is perpendicular in the touch current cases. Further illustrations are in Figure D.2, Figure F.6, Figure F.9, and in particular Figure F.10 which shows the effect of the formula of current continuity. In general:

a) the strongest coupling is to a tissue object with its major axis parallel with the direction of a homogeneous B flux, see Figure D.3;

b) to the first order, the maximum induced E field amplitude coupling is inversely proportional to the circumference of a simple round object located as in a) above;

c) the coupling is reduced with smaller curvature of the B flux and stronger decay rate of it away from the source;

d) there is invariably a minimum induced E field in the central regions of a tissue object and always a maximum in the surface region of a reasonably homogeneous object.

NOTE 1 A homogeneous B field is in principle not a nearfield as defined in this Technical Specification, but is useful as a basis for the comparisons in Annex D.

NOTE 2 **Magnetic nearfield** conditions as addressed in this Technical Specification are not considered in the ICNIRP guidelines and IEEE standards; see Annex A.

B.3 Coupling of a homogeneous B field to homogeneous objects with simple geometries

What happens can, for simplicity, be investigated with a Helmholtz coil, as described in Annex D.

- the conductivity is so low that wave energy penetration depth effects do not occur – i.e. there is no secondary (counteracting) internal B fields by any currents caused by the induced E field;

- the conductivity is so high, and the size of the bodypart is so large, that an efficient reflection away of the impinging external E field from the source occurs, with no significant internal power absorption except in extreme situations.
- the relationship $E = \pi R \cdot f \cdot B$ inserted into Formula (1) holds for a long circular cylinder with radius R in a homogeneous axial B field if this B field is not influenced by the object. The **coupling value** C thus then becomes πR and is frequency independent.

NOTE As an example from the numerical computations described in Clause D.1, C becomes 0,302 for a 200 mm diameter sphere, using Formula (1). The quotient thus becomes $0{,}302/0{,}1\pi = 0{,}96$. The deviation is due to the sphere having a curvature in all three dimensions. It is thus expected that the coupling factor to a long circular cylinder with the same diameter is about 4 % higher.

When the flux decays over the object, C typically becomes smaller than in a homogeneous flux, since it influences the back side more weakly, reducing the overall circulating current amplitude. However, conditions resulting in an increase of C can occur under certain conditions; see Clause E.5 and Table E.1. It shall then be observed that the main direction if the flux can change in relation to the main surface of the object if moved linearly away from the flux source. There is then also a problem with determination of the actual C since the flux amplitude varies. For a straight conductor and a coil, it becomes necessary to instead use the source current and geometry, and then calculate or model the flux in the region of interest; see Annex F.

B.4 Starting points for numerical modelling

B.4.1 Relevant bodyparts

Since the curvature R_{osc} of a homogeneous magnetic field is infinite and the magnetic field intensity decays as the radial distance from a long straight conductor (Formula B.2) and the cube of the radial distance from a loop at a distance (Formula B.3), wholebody exposure from a **magnetic nearfield** can in practice be excluded, thus limiting the significant nearfield influences to only parts of the head and trunk, and to arms, hands and fingers.

NOTE Reference objects for numerical modelling, representing typical bodyparts, are given in Annex C.

B.4.2 The use of external B field and internal power density in numerical modelling

Formulas (1), (B.4) and (B.5) show that there is a linear proportionality between the inducing B field strength and the induced E field strength, with frequency as a linear parameter. Rather than using the conductor current and its circuit geometry as a start for the system analysis, using measured B values is preferred in cases with complicated and large source geometries as well as with objects nearby which disturb the B field pattern. This is also since such values are in practice not influenced by the presence of bodyparts. However, if these conductivities result in a power deposition caused by external displacement current sources being enhanced by frequency upscaling in numerical modelling, quantifying and separating those effects from the magnetically induced effects becomes necessary. This can be by methods described in Annex H.

Direct extraction of the internal $|E|$ field is typically not preferred, since there is a need to include the conductivity parameter, and the external E field is invariably magnitudes higher than the internal. Obtaining the *in situ* E values by modelling is instead typically by selecting the power density p (per volume unit and averaged over a cycle or taken as amplitude), and then in the result using the relationship, under conditions of a single frequency time-harmonic pattern:

$$p_{\text{eff}} = \frac{\sigma |E_{\max}|^2}{2} \quad p_{\max} = \sigma E_{\max}{}^2 \tag{B.7}$$

where E is in Vm^{-1} and p is in Wm^{-3}.

NOTE Calculations of **SAR** values require knowledge of the specific densities of the tissues; see the note to the **SAR** definition in 3.1.11.

Annex C
(normative)

Reference objects representing parts of the body: tissue conductivities

C.1 Reference bodyparts

C.1.1 General

Five totally realistic overall model geometries are used, representing a finger, a wrist/arm, and a hand. No head model is specified, since it is assumed that limbs will invariably be closer to the source and stronger *in situ* E fields may be induced by magnetic non-nearfields.

The conductivites of the test loads are set as to not result in any energy penetration depth issues; see Annex H.

Dielectric data and their uncertainties shall be included in the overall assessments dealt with in Clause 8. It shall be specified what overall tissue combination is used in the numerical modelling.

C.1.2 The wrist/arm models

The shape is simply a 350 mm long 50 mm (wrist) or 80 mm diameter (arm) circular cylinder. Its primary use is for basic investigations such as in Annex E.

C.1.3 The hand model with tight fingers

The shape consists of an inner rectangular block with dimensions 140 mm × 80 mm × 20 mm, plus semi-elliptical ends with the same thickness and radii 40 mm and 20 mm. There are outer semicircular edge regions protruding 10 mm out from all sides. The outline is shown in e.g. Figure E.4 and Figure E.5.

C.1.4 The hand model with spread-out fingers

The shape is a combination of a shortened hand model and five finger models as in C.1.5 cut by the hand model. The hand model is as in C.1.3 but with a 60 mm instead of 120 mm inner rectangular block and five fingers with the mid one ending 20 mm from the reduced hand model centre. The axis of rotation is 30 mm on the other side of this centre, and the angles of rotation from that point is 15°. The outline is shown in Figure F.10.

C.1.5 The finger model

This consists of a diameter 17 mm and 100 mm long circular cylinder, with added hemispherical ends. The overall length is thus 117 mm.

C.2 Dielectric properties of human tissues

C.2.1 General data for assessments

The electromagnetic properties of the tissues of the subjected parts of the body are important for the assessments and calculations of **SAR** values. The average values of electrical conductivity σ for a human body to be used is 0,2 Sm^{-1} for frequencies up to 100 kHz and 0,5 Sm-1 for frequencies higher than 1 MHz. The formula $\sigma = 0{,}2 + 0{,}3 \cdot {}^{10}\log(f/10^5)$ Sm^{-1} is applicable between these frequencies. These average values are recommended only for assessment procedures using very simplified body models with homogeneous electrical conductivity and it is to be noted that the corresponding conductivities for nerves are half or less of that of the body average.

C.2.2 Inner parts of the body

Table C.1 – Examples of dielectric data of human tissues at normal body temperature

Tissue type	Real relative permittivity ε'	Equivalent conductivity σ [Sm^{-1}]	Equivalent dielectric loss factor ε'' [1]
—	f = 10 k; 100 k; 1 M; 6 M	f = 10 k; 100 k; 1 M; 6 M	f = 10 k; 100 k; 1 M; 6 M
Blood	≈4k; ≈4k; ≈3k; ≈600	0,8; 0,8; 0,8; 1,0	1,44M; 144k; 14k; 2900
Breast fat	500; 60; 20; 12	0,025; 0,025; 0,025; 0,030	45k; 4500; 450; 90
Gray matter	20 000; 4 000; 1 000; 300	0,12; 0,14; 0,18; 0,25	216k; 25k; 3 200; 740
White matter	9 000; 2 000; 800; 200	0,07; 0,08; 0,10; 0,15	126k; 14k; 1 750; 440
Muscle	50 000; 10 000; 2 000; 200	0,4; 0,5; 0,6; 0,8	720k; 90k; 11k; 2 450

The set of data from the Camelia Gabriel group are universally used as basic reference. So some such selected data are given in Table C.1. Frequencies are in Hz. k = 1 000; M = 1 000 000.

NOTE 1 Data exist in Annex B of EN 50444:2008, but are only for the conductivity and refer to a US web source no longer available.

NOTE 2 There is typically a need for frequency upscaling In FDTD numerical modelling. The factors then to consider for the choice of proper equivalent dielectric data are dealt with in Annex H.

C.2.3 Skin data

Data (also for the substances in Table C.1) are available from the Italian National Research Council Institute of Applied Physics “Nello Carrara”, Florence Italy, and shall be used.

As a first example dry skin at 10 kHz has σ = 0,000 20 Sm^{-1} and ε' = 1 135. Using $\varepsilon'' = \sigma/2\pi f\varepsilon_0$ one obtains ε'' ≈ 360 and an effective ε ≈ 1 200. These data clearly indicate that the skin is shorted-out by the adjacent tissue having σ higher than 0,05 even for nerves.

As a second example wet skin at 10 kHz has σ = 0,003 0 Sm^{-1} and ε' = 29 000. One obtains ε'' ≈ 5 400 and an effective ε ≈ 29 500. This corresponds to an equivalent conductivity 0,17. These data again indicate that the skin is essentially shorted-out by the adjacent tissue.

Annex D
(informative)

Results of numerical modelling with objects in a Helmholtz coil and at a long straight conductor

D.1 General and a large Helmholtz coil scenario with a diameter 200 mm sphere – FDTD 3D modelling

A homogeneous magnetic field provides results which can also be calculated by analytical methods. The solution for a long circular cylinder with radius R and axis parallel with the magnetic B field at frequency f becomes very simple: the maximal internal E field is at the periphery and becomes $\pi \cdot R \cdot B \cdot f$.

NOTE 1 This fact is used as reference for the 2D model calculations in IEC 62226-2-1:2004, where a 2D dimensionless coupling factor K (called K_{2D} in this Technical Specification) is introduced and defined as C divided by $\pi \cdot R$. The 2D model in IEC 62226-2-1:2004 is represented by true 3D scenarios with an infinitely long mathematically cylindrical object in a B field having only a component in its axial direction varying with position in the plane perpendicular to the axis. A 3D wire is thus represented by an axially infinitely long conductor sheath with current flowing only perpendicularly to the object axis. In spite of this practical deficiency, such 2D models provide valuable insights into the behaviour of the induced E field by an external B field.

The Helmholtz coil pair consists of two horizontal large circular conductors with cross section 6 mm × 6 mm with 1 190 mm centre diameters, with centres located 595 mm vertically from each other at the same axis. Each loop is fed from a small coaxial pocket, with an equal receiving pocket back to back. There is of course an impedance mismatch at the feeds, but the “actual” magnetic fields are extracted. The operating frequency is 6 MHz, for reducing the runtime of the large scenario (26 million voxels with 2 mm × 2 mm × 2 mm resolution in the critical regions including the mid parts of the sphere). Its conductivity is set to 1,055 Sm^{-1}. This is higher than for normal tissue and chosen due to the frequency upscaling (see Annex H), but will typically result also in a capacitively coupled surface power deposition. However, that effect becomes insignificant in a Helmholtz coil. Results were obtained with the commercially available QuickWave[2] FDTD software.

Figure D.1 shows the strongly dominating z-directed magnetic field amplitude in a large volume in the central vertical y plane. As expected, it is quite constant in the region of the sphere, which is marked by the black circle. The extracted B field amplitude is 441 nT. Figure D.2 shows the power density pattern. The ring-shaped maximal power density in the equatorial region is 0,672 $W \cdot m^{-3}$, corresponding to 0,798 $V \cdot m^{-1}$. Using Formula (1) one obtains $C \approx 0{,}302$ m. The C value uncertainty is less than ±1 %, due to the small voxels.

NOTE 2 Theoretical aspects on this scenario are discussed in Clause B.2.

2 QuickWave FDTD software by QWED Sp. z. o. o. (www.qwed.eu) is an example of a suitable numerical modelling software available commercially. This information is given for the convenience of users of this document and does not constitute an endorsement by IEC of this product. All colour figures in this and the following Annexes, except E.8 and F.1, were obtained by this software.

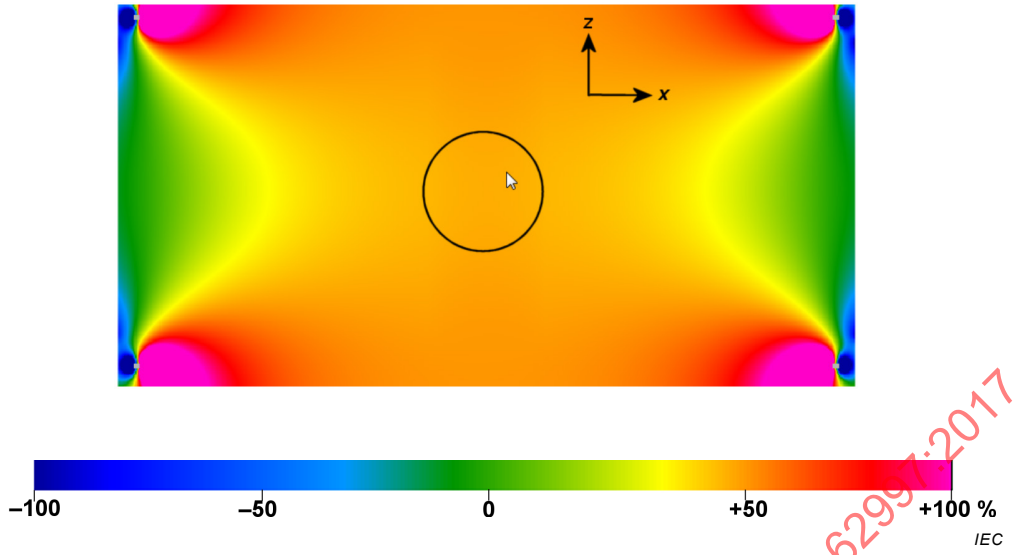

Figure D.1 – The z-directed magnetic field momentaneous maximal amplitude in the central y plane of the Helmholtz coil with the conductive 200 mm diameter sphere

D.2 Other reference objects in the Helmholtz coil – FDTD 3D modelling

D.2.1 The scenario

The sphere is now replaced by several centrally located bodypart objects as defined in Annex C and having the same conductivity as the sphere in Figure D.1. Their orientation is as shown in Figure D.3. Simultaneous numerical modelling is possible since the mutual coupling and influence on the magnetic field are insignificant. The frequency is still 6 MHz.

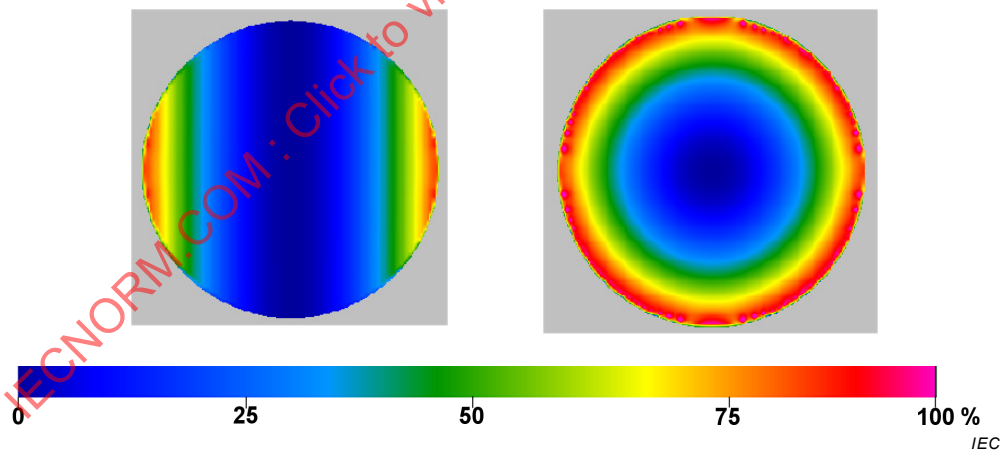

Figure D.2 – The power density patterns in the central y plane (left) and central z (equatorial) plane of the 200 mm diameter sphere

D.2.2 Numerical modelling results with smaller spheres

This was with 100 mm and 50 mm diameter spheres. Comparisons were made with the power density at the corresponding distances from the centre of the 200 mm sphere. All results were fully consistent with the induced E field being proportional to the distance from the sphere centre, which indicates the correctness of the theory under conditions of homogeneous B field in rotationally symmetric objects with axis in the B field direction, and also that the conductivity was appropriately chosen in view of the constraints described in Annex H.

D.2.3 Numerical results with other objects

The composite Figure D.3 gives an overview of the objects and their C values in the mid z plane of the Helmholtz coil. The colour scaling is different in order to see the patterns.

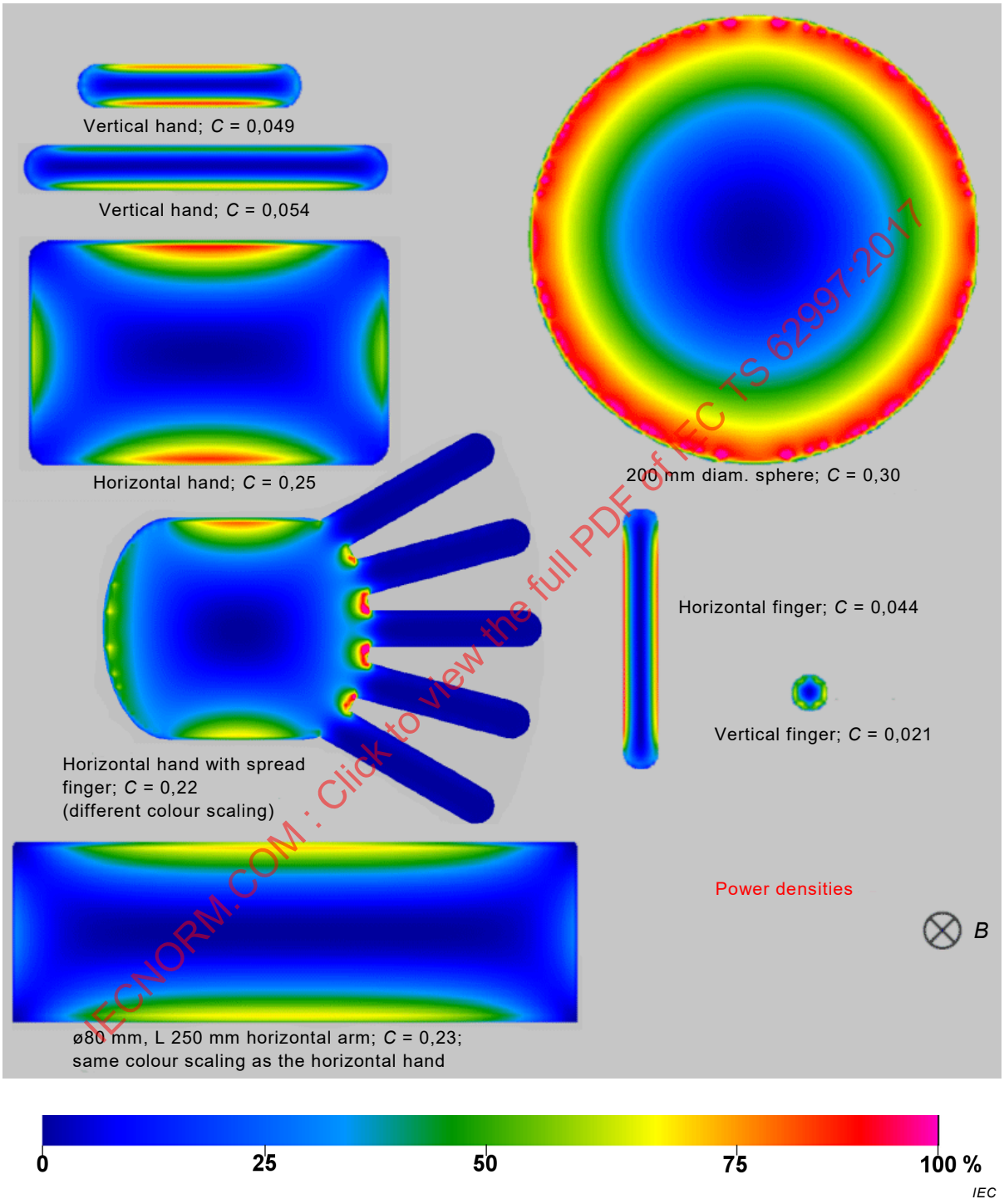

Figure D.3 – The power density patterns in the central z plane of the reference objects, with maximal C values in m

NOTE Comparing the relationship of C being proportional to the object radius R with the numerical results for the sphere and vertical finger, the deviation as obtained by the numerical modelling is less than 15 %.

Annex E
(informative)

Numerical FDTD modelling with objects at a long straight wire conductor

E.1 Scenario and general information

The scenario now consists of a 1 425 mm long wire with 1 mm diameter, fed by a small coaxial pocket and having an equal receiving pocket in the other end; see Figure E.1. The current source (black line) is to the right in the figure. The scenario boundary on the four sides except those with the wire ends is a 60 mm thick layer of an artificial absorbing material (dark yellow in the Figure) with $\varepsilon' = \mu' = 1$ and $\sigma = \sigma_\mu = 0{,}05$ Sm^{-1} , where $\sigma_\mu = 2\pi f \mu_0 \mu''$. This material is 120 mm thick at the wire ends and thus covers them. Inside these 120 mm layers there are additional 60 mm thick absorbing layers (magenta in the figure) with ε' and $\mu' = 1$ and $\sigma = \sigma_\mu = 0{,}002\ 5$ Sm^{-1}.

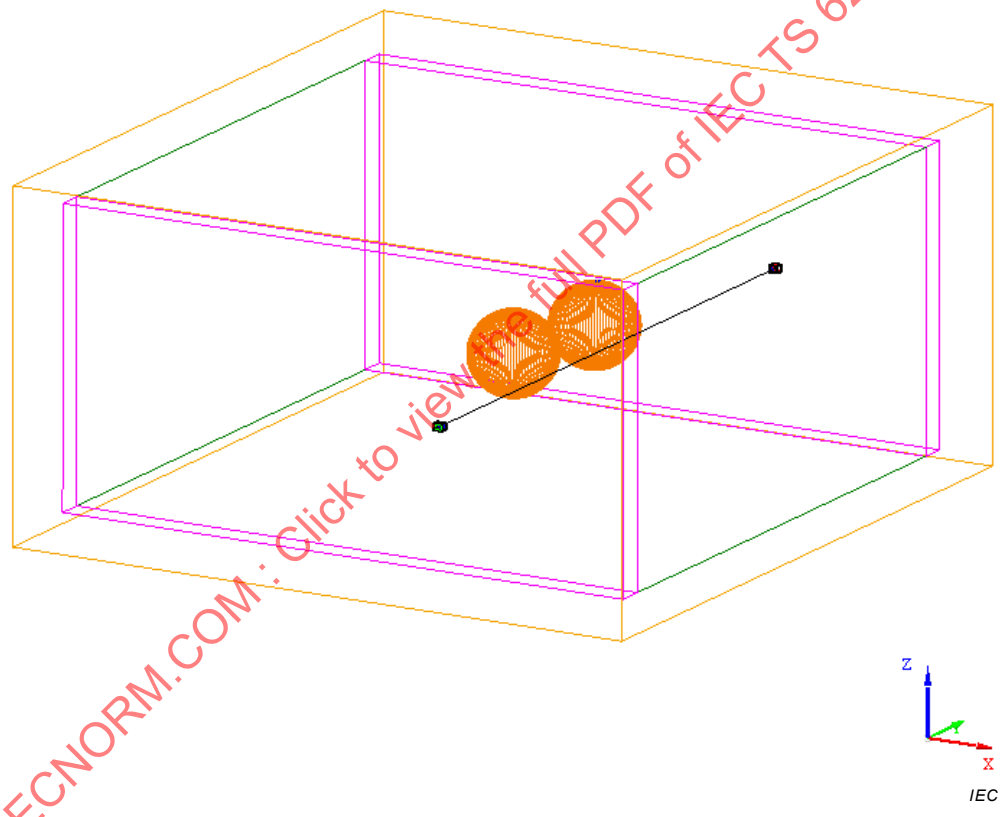

Figure E.1 – Long straight wire scenario

Figure E.2 shows two 200 mm diameter spheres with their nearest surfaces 10 mm and 50 mm from the wire and centred in the z plane of the wire. The sphere electrical conductivity is initially set to 1,055 Sm^{-1} and the operating frequency to 6 MHz. The reason for the use of these complicated absorbing layers is that **magnetic nearfields** cannot be absorbed by conventional absorbing boundaries (such as the MUR approximation) used in numerical FDTD techniques.

There is now an interaction between the curvature of the object as well as that of the B field, and also modifications of the **coupling value** C due to the field decay with distance from the wire. The excitation of the wire results also in a radial E field. Unless minimised by conductivity increases with frequency upscaling, a significant capacitively coupled surface power deposition will occur, due to redistribution of the induced charges. The phenomenon is

in practice noticeable only with sharp conductive parts very close to the conductor and can be separated out from the magnetically induced E field; see Clause H.4.

The power density relative scaling in all images in this Annex E are as shown in Figure E.2. The electric field scaling in the right image in Figure E.10 is the same.

E.2 Two 200 mm diameter spheres

The scenario with two 200 mm diameter spheres is illustrated in Figure E.1. The power deposition pattern becomes distorted with σ = 1,055 Sm^{-1}. Therefore, σ = 20 Sm^{-1} was chosen; see Figure E.2. This is so high that no direct influence by any external electric field occurs. According to Formula (H.3) the energy penetration depth d_p becomes about 23 mm. This is sufficiently large for the purpose of characterising the electric field deposition in the shallow maximum region of the object.

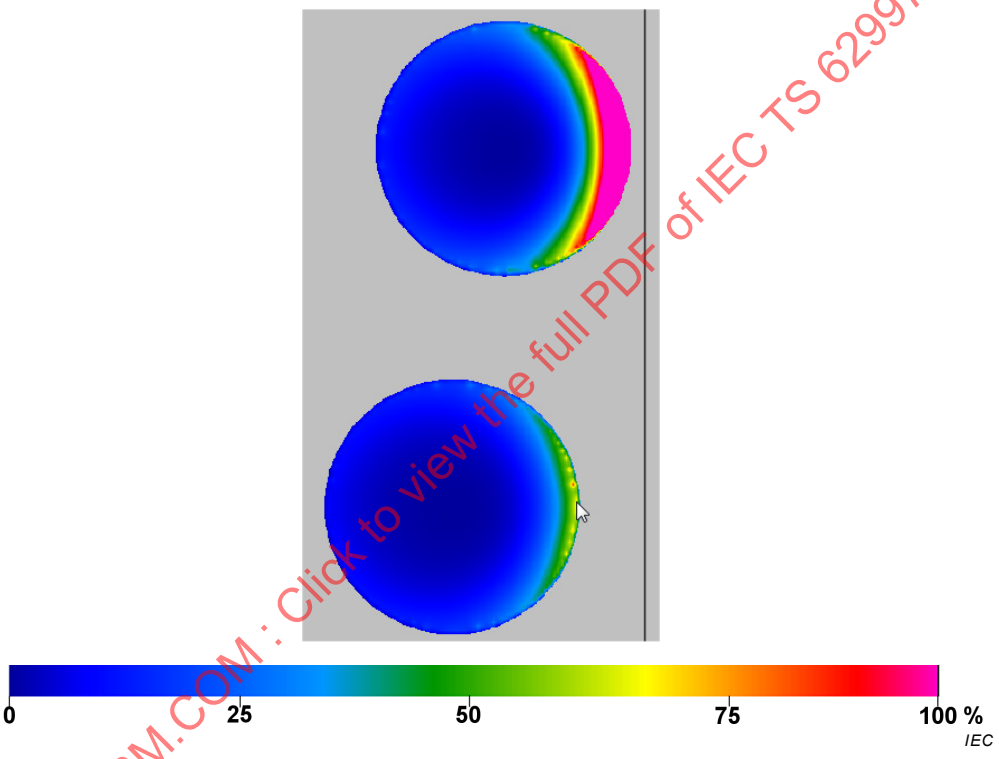

Figure E.2 – Power deposition patterns in the central z planes of the two spheres at 10 mm and 20 mm away from the sphere axis; σ = 20 Sm^{-1}

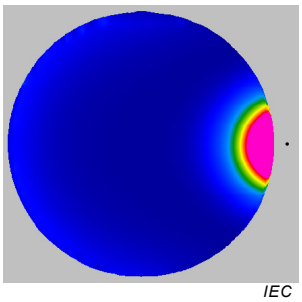

Figure E.3 – Power deposition pattern in the central y plane of the sphere at 10 mm distance from the wire axis; σ = 20 Sm^{-1}

It is seen that the power deposition pattern is wider in the plane of the wire (Figure E.2) than in the perpendicular plane (Figure E.3).

The maximum power density in the sphere at 10 mm distance was 2,5 times higher than at the magenta boundary, which is 20 mm inwards from the surface.

Using the maximum power density and *z*-directed B field values (see Figure E.1 on co-ordinates) in the same locations just outside the spheres, the C value at the 10 mm distance becomes 0,084 m. At the 50 mm distance it becomes 0,150 m.

The reduced **coupling value** C compared with the Helmholtz coil case ($C \approx 0{,}302$ m) is due to the smaller object part influenced by the strongest B field and its faster decay away from the wire axis, as well as on its curvature. The C value at infinite distance from the wire should theoretically approach the value in the Helmholtz coil, see Figure D.3.

E.3 The hand model with tight fingers at different distances from the wire – FDTD modelling

E.3.1 General information and scenario

The basic scenario outline is the same as in Figure E.1, but the overall height was increased for the larger distances between the wire and the hand model, and the wire diameter was only 0,5 mm. The model was centred over the wire with its long sides parallel to it (y-directed). The distance of the underside to the wire axis is the parameter, and varies from 2,5 mm to 200 mm.

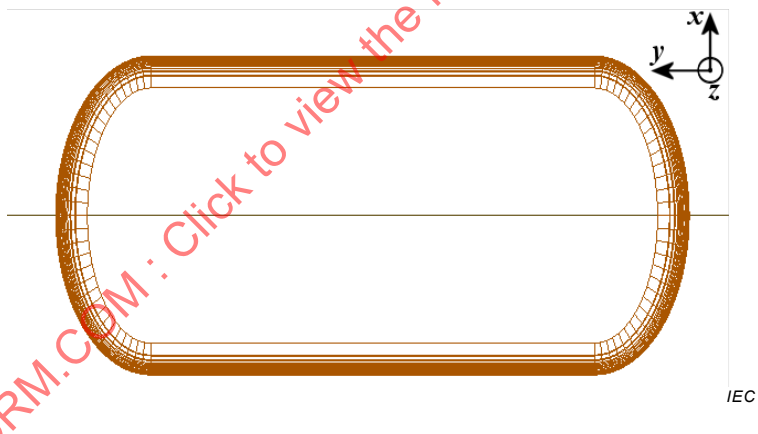

Figure E.4 – Scenario with the hand model above the wire axis

E.3.2 Modelling results – power deposition patterns

Figure E.5 to Figure E.7 show the power deposition in the central y plane and the bottom plane, at various heights.

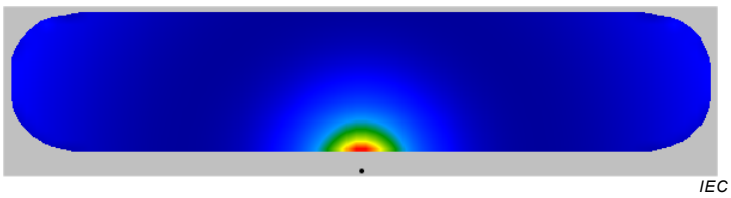

Figure E.5 – Power density in the hand model 2,5 mm above the wire axis

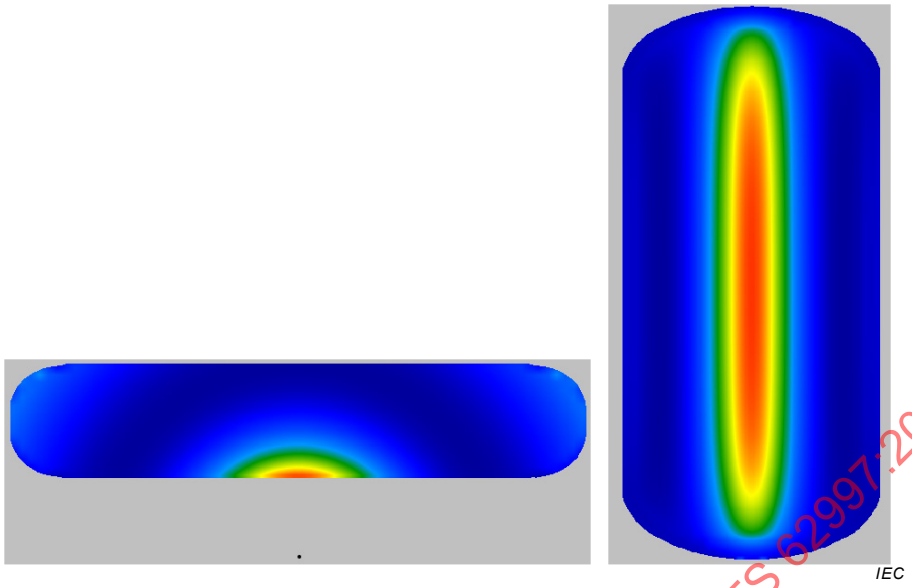

Figure E.6 – Power density in the hand model 14 mm above the wire axis

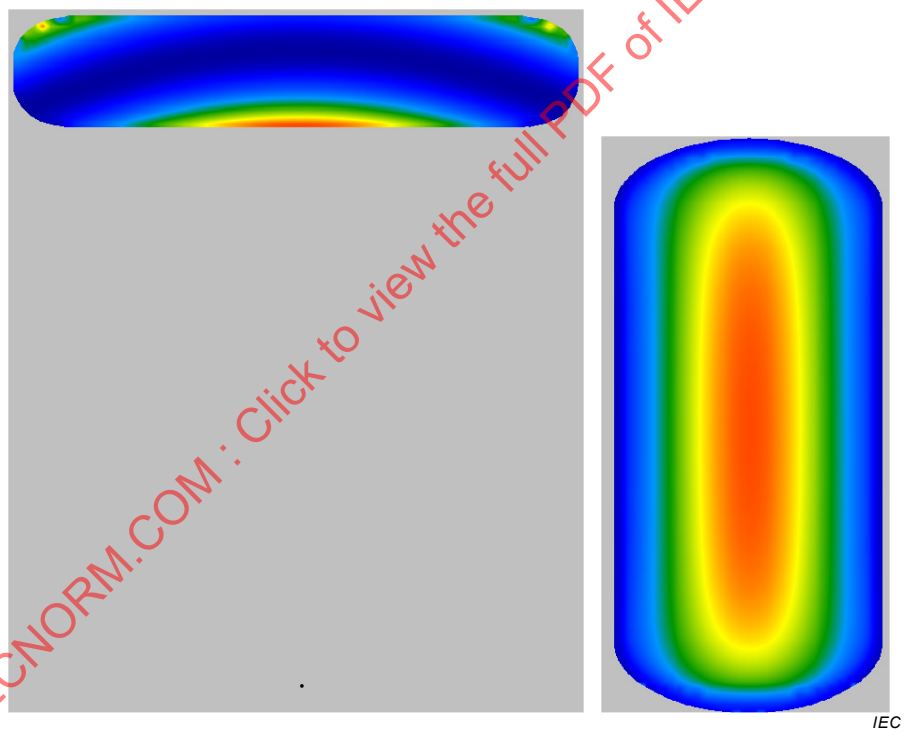

Figure E.7 – Power density in the hand model 100 mm above the wire axis

It is seen that a current return path exists, as more clearly demonstrated in Figure E.7 and Figure E.8.

E.4 The hand model with tight fingers at 100 mm from the wire – Flux® 12[3] FEM modelling

NOTE 1 The numerical modelling FEM software does in principle not require a complete enclosed scenario as does FDTD software. The resulting quasi-3D scenario becomes easier to construct and runs faster since the FDTD timestep stability criterion is not needed. An infinitely long conductor can therefore be used.

NOTE 2 The modelling result in Clause E.4 is intended only to basically confirm the results of the FDTD modelling in this Technical Specification.

IEC

Figure E.8 – Current density in the central cross section of the hand model at 9 mm from the wire – Flux® 12 FEM modelling

NOTE 3 The colour scaling in Figure E.8 is with white/yellow being maximal and dark blue/black minimal.

Figure E.8 is compared with Figure E.6 and a good similarity is observed. However, the actual and very fast modelling was made in 2D with an enforced overall null current; see Formula (B.6) and Note 1 in Clause D.1.

E.5 Coupling data and analysis for the hand model with tight fingers above the wire – FDTD modelling

Table E.1 shows the calculated C values obtained by the FDTD modelling and Formula (1). A high conductivity σ = 20 Sm^{-1} was used for minimising any external electric field influences; see Clause E.2.

Table E.1 – Coupling factors for the hand model with tight fingers at various heights above the wire axis

Distance from the wire axis to the underside of the object (mm)	C **in** E **maximum voxel** (m, rounded-off)	**Remarks: radial extension** Δ (mm) **from the surface where the power density is halved**
2,5	0,038	$\Delta \approx 2$ mm
3,5	0,044	$\Delta \approx 2½$ mm
5	0,056	$\Delta \approx 3$ mm
9	0,067	$\Delta \approx 4$ mm
14	0,073	$\Delta \approx 4$ mm
30	0,083	$\Delta \approx 5$ mm
100	0,082	$\Delta \approx 4,5$ mm
(∞)	0,054	From Figure D.2 for vertical hand in Helmholtz coil; $\Delta \approx 4$ mm

NOTE **CGCR** values are given in Figure G.1.

Table E.1 shows that the C value is smallest for the hand very close to the wire, due to the stronger field curvature there. The reason for the C values being slightly larger for the larger distances in Table E.1 than in a homogeneous field is that the symmetric (equal) but

[3] Flux® 12 FEM software by CEDRAT (www.cedrat.com), owned by Altair Engineering, Inc., is an example of a suitable numerical modelling software available commercially. This information is given for the convenience of users of this document and does not constitute an endorsement by IEC of this product.

oppositely directed current paths on both sides in the homogeneous field case no longer exist, so that there is less reduction of the current in the facing flat side than that in the opposite flat side. The magnetic field spatial decay rate can thus be such with certain object shapes that the C value has a maximum for a quite small B field spatial decay rate, and not with such a homogeneous field. Obviously, this maximum is roughly for 30 mm to 100 mm distance in this case. The unequal power deposition pattern on the major sides of the hand model is still very strong at 100 mm distance; see Figure E.7.

E.6 Coupling data and analysis for the wrist/arm model above the wire

The arm diameter is 60 mm and the scenario is shown in Figure E.9. The distance between the wire centre and the arm underside is 10 mm. These data are of interest, since the result of 2D numerical modelling is given in Table D.1 in IEC 62822-2:2016.

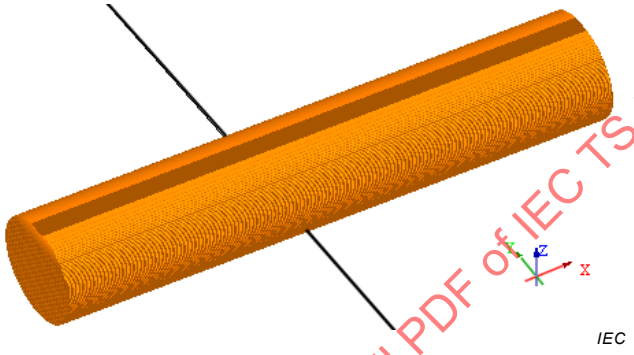

Figure E.9 – Wrist/arm model above a long straight wire

The power density and E field patterns are shown in Figure E.10.

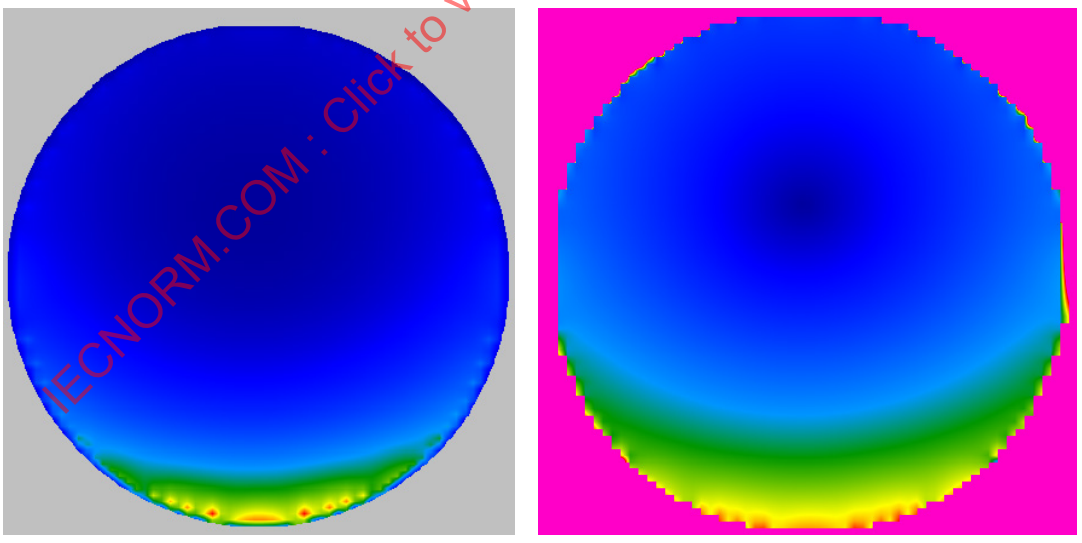

Figure E.10 – Linear power density (left, power scaling) and electric field amplitude (linear scale) in the x plane of wrist/arm model 10 mm straight above a long straight wire

NOTE The electric field strength is much higher outside than inside the object, due to the very high effective permittivity of the latter. The external field is therefore oversaturated in the image.

Using the magnetic field strength at the nearest part to the wire, and the E field strength there, one obtains C = 0,053 m. This is lower than the interpolated value for the hand:

C = 0,068 m. Using the coupling factor K_{2D} as used in IEC 62822-2:2016 for the same but 2D scenario addressed in Annex D, one obtains $C \approx 0{,}383 \cdot \pi \cdot 0{,}03 \approx 0{,}036$ m. The reason for the difference is again, as addressed in Clause E.5, that the 2D scenario 2D current sheath improves the balance between the oppositely directed current paths in the object, in comparison with that caused by the 1D wire in the true 3D modelling.

Annex F
(informative)

Numerical modelling and volunteer experiments with the hand models at a coil

F.1 General and on the B field amplitude

The power density relative scaling in all images in Annex F are as shown in Figure F.3. The electric field scaling is shown in Figure F.6, Figure F.8, and Figure F.18.

Some B field properties at single-turn coils are described by Formulas (B.3) and (B.4). The magnetic field is illustrated by Figure F.1, obtained by FEM modelling of a coil with 137 mm outer dimeter and 10 mm × 7 mm conductor cross section as used throughout in this Annex F. The distance between the lines indicates the field strength while their directions are indicated by the field vector; the intensity is also colourscaled.

The electrical conductivity σ of the objects is 1; 10 or 20 Sm^{-1}, in consideration of the frequency upscaling; see Annex H. The operating frequency with the FDTD modelling was 6 MHz, throughout.

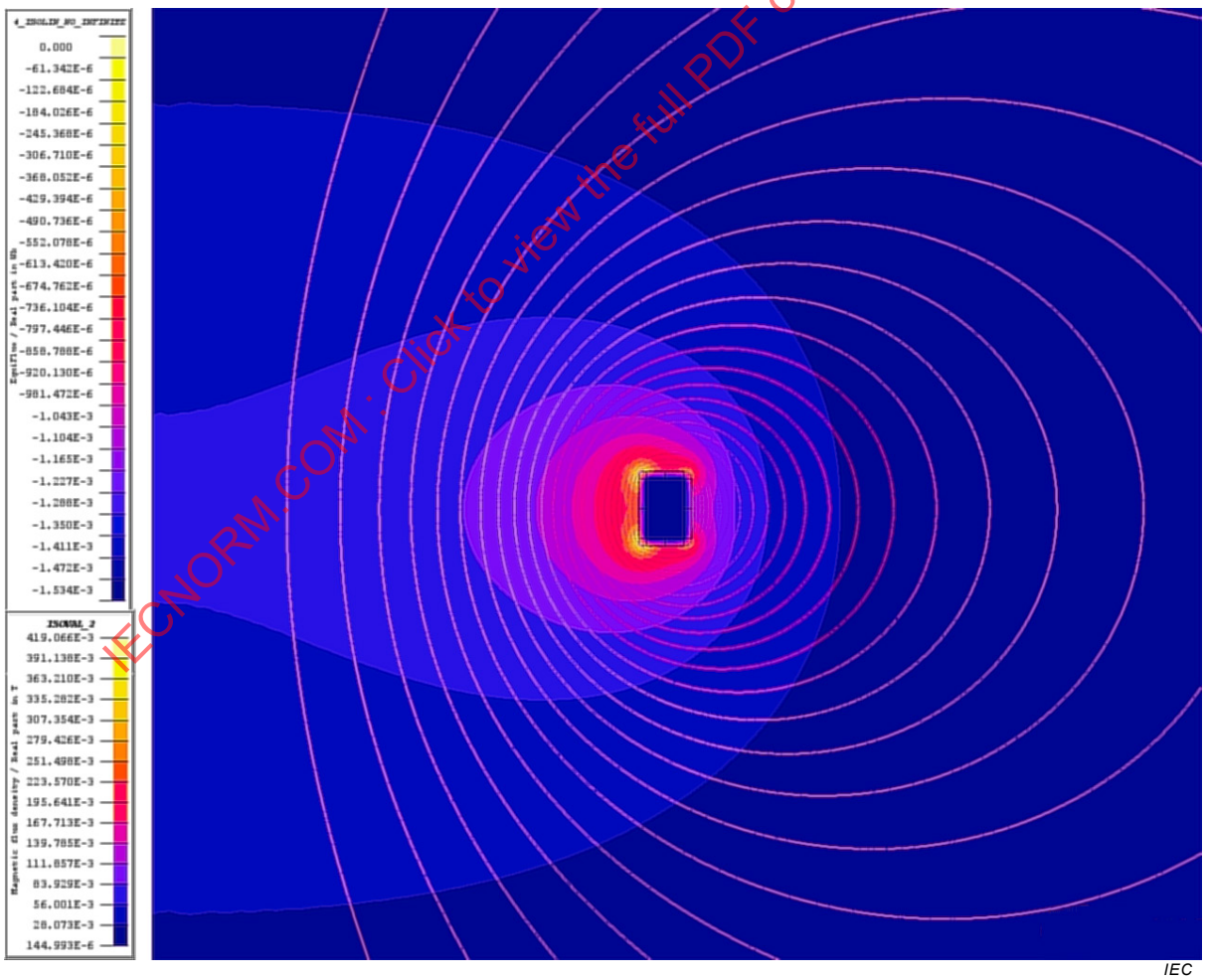

Figure F.1 – Illustration of the B field at a single turn coil, with the coil centre at the left margin of the image – Flux® 12 FEM modelling

NOTE The colour scaling in Figure F.1 is with white/yellow being maximal and dark blue/black minimal.

The characterisation of the B field at an object such as a finger at a **POI** near the coil is more complicated than with a wire, since the field curvature and amplitude change with position in a more complicated way. At a long straight conductor both the B field curvature R_{osc} and the B vector amplitude are inversely proportional to the distance to the **POI**. The B vector direction is in the φ (angular) direction. Furthermore, the coil is loaded in operation in an induction equipment, but the approaching bodypart can also be in empty operation.

Two measurement methods are recommended, provided the loading does not change the external field characteristics appreciably:

a) Measurement of the coil current and using the coil dimensions and Formula (B.2) or (B.3) to determine the B field characteristics.

b) Measuring the B field at the coil axis (spherical co-ordinate θ = 0° or 180°) and using that as a B field amplitude scaling parameter, with Formula (B.2) and data from this Annex or elsewhere.

The use of these methods is addressed in 6.2, using data from Annex F.

A direct way to eliminate a number of uncertainty factors is to use the volunteer test method in 6.3, together with the CGCR method described in 6.2.

F.2 The hand model with tight fingers 2 mm, 4 mm, 6 mm and 50 mm above the coil and with its right side above the coil axis – FDTD modelling

F.2.1 The scenario

A coil in F.1 with mesh size 1 mm × 1 mm was used, with FDTD modelling. The feed/receiving coaxial ends are in the same metal coaxial line enclosure to the right in Figure E.1.

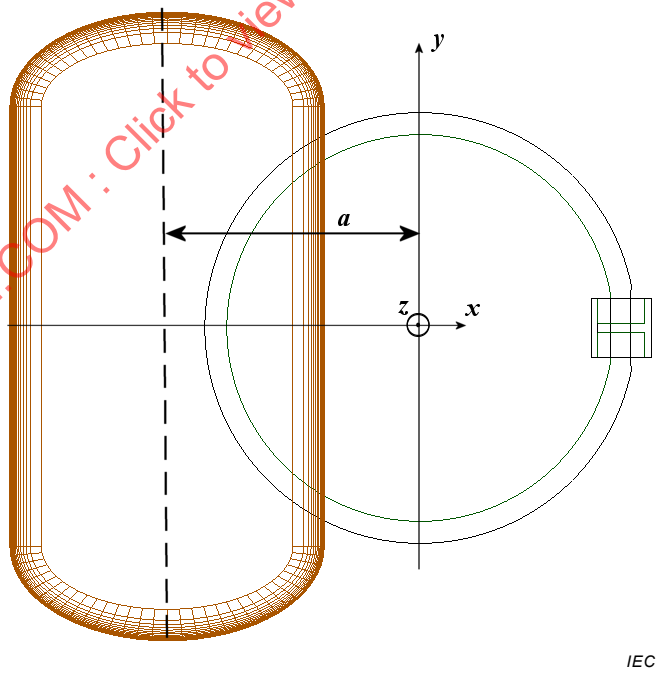

Figure F.2 – Hand above the coil scenario

The distance between the coil and hand model in the *z* direction is between the coil topside and the hand underside. The sideways hand displacement a is shown in Figure F.2.

F.2.2 Modelling results

Some power density patterns are shown in Figure F.3 to Figure F.5, in the σ =10 Sm^{-1} case.

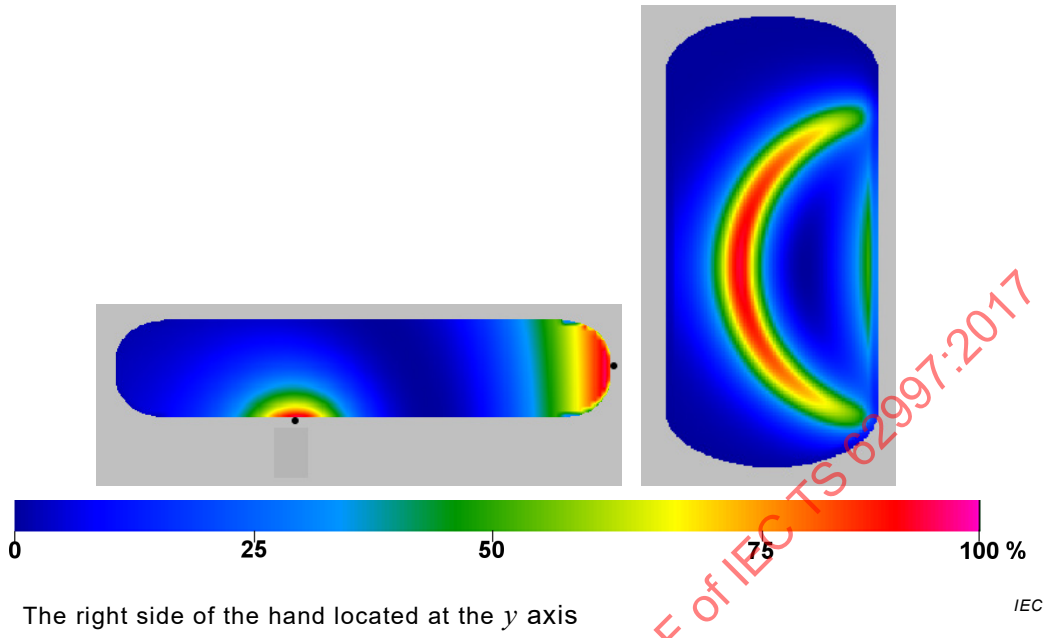

Figure F.3 – Power density pattern in the central vertical plane and in the bottom 1 mm layer of the hand model, z = 2 mm above the top of the coil; a = –51 mm

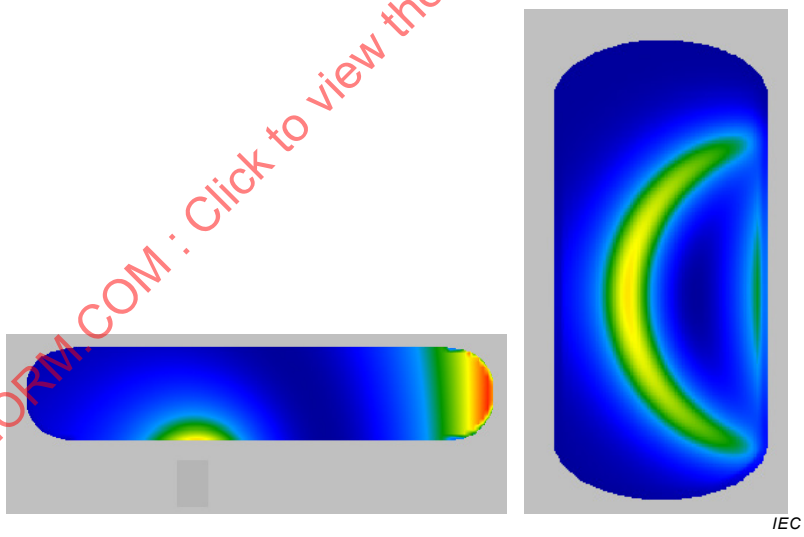

Figure F.4 – Power density pattern in the central vertical plane and in the bottom 1 mm layer of the hand model, z = 4 mm; a = –51 mm

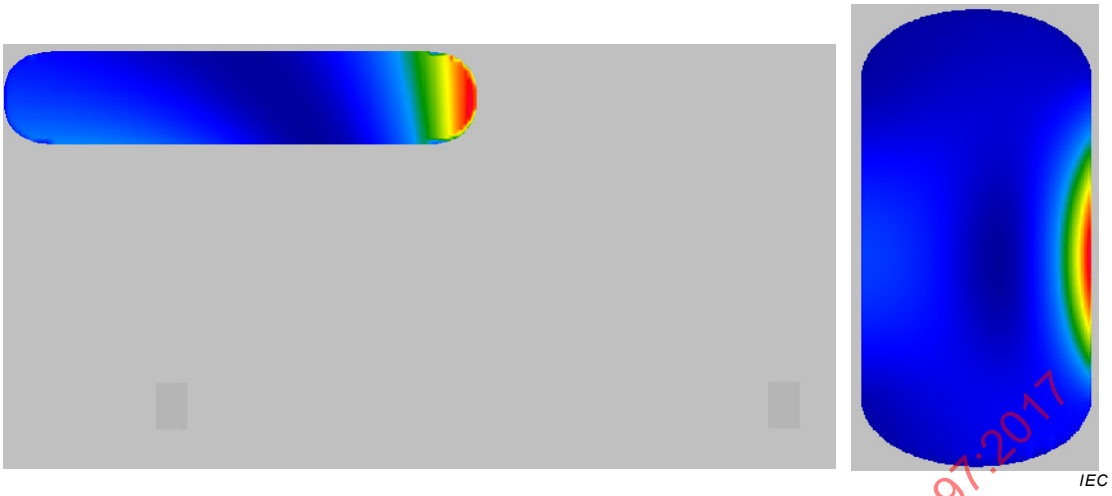

Figure F.5 – Power density pattern in the central vertical plane and in the bottom 1 mm layer of the hand model, z = 50 mm; a = –51 mm

The magnetic field at the coil centre was 15,9 µT. It was 46,7 µT at the hand underside 2 mm above the coil opposite the feed and at the power density maximum. It was 14,2 µT at the other coupling maximum at the hand side. These points are shown in the left Figure F.3.

The maximum power density in the z = 2 mm case was 0,367 W/dm^3 in the bottom maximum and 0,350 W/dm^3 at the hand side; see Figure F.3. In the scenario in Figure F.4 with z = 4 mm the corresponding values were 0,280 W/dm^3 and 0,349 W/dm^3, respectively. With z = 6 mm (shown with workload in Figure F.14) the bottom (curved) value was 0,219 W/dm^3 and it was 0,320 W/dm^3 at the hand side. With 50 mm distance in Figure F.5 the power density was 0,0365 W/dm^3, i.e. about 9 times smaller, so the colour scaling of the power density in that figure was reduced by a factor 9.

The induced current in objects such as the hand model forms a closed loop which thus has a null somewhere in the central region. This is illustrated by Figure F.6.

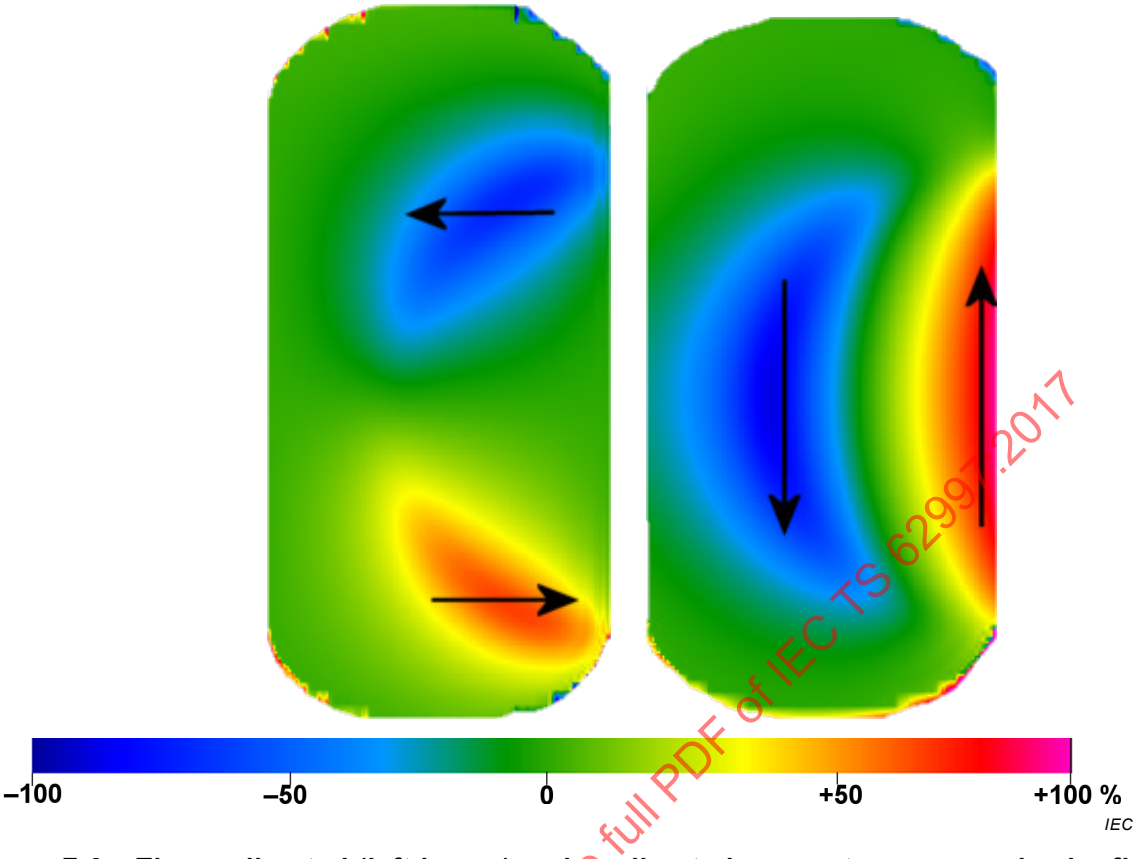

Figure F.6 – The ±*x*-directed (left image) and ±*y*-directed momentaneous maximal E field at the hand underside, z = 4 mm; a = –51 mm

The amplitude scale is the same in both images in Figure F.6. It is seen that the field direction changes considerably and can be said to be approximately elliptical. The pattern is likely to weaken the nerve reactions, since the field will not be directed along the sensing nerves for any longer distance as is the case with typical contact current paths. Furthermore, a quite small relative volume of the hand has the strong E field due to the nearfield characteristics: only about 10 % of the overall volume of about 225 cm^3.

The asymmetry of the scenario results in a current path which is not controlled by the coil nearby, i.e. at the hand side, to spread out and then be more concentrated – maximal – at the hand edge. This is clearly seen in Figure F.5.

The spatial integration for immediate nerve and muscle reactions in fingers, hands and arms specified in 6.2 shall be applied and is shown in Figure F.8 and Figure F.9, in the σ = 10 Sm^{-1} case.

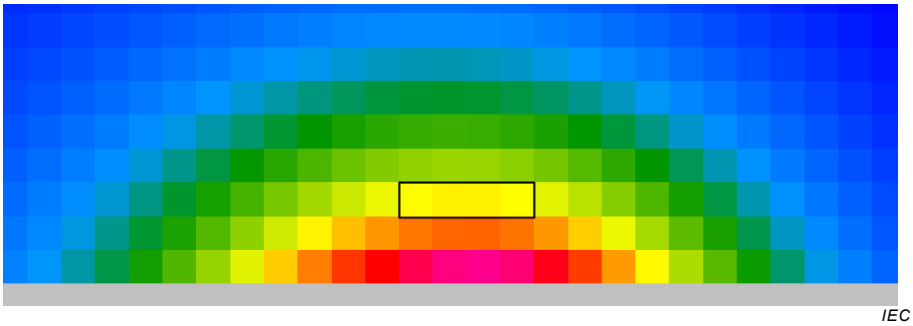

Figure F.7 – The local power density pattern of the condition in Figure F.3, showing the 1 mm × 1 mm voxel size and the 5 mm^2 integration region 2 mm above the hand underside

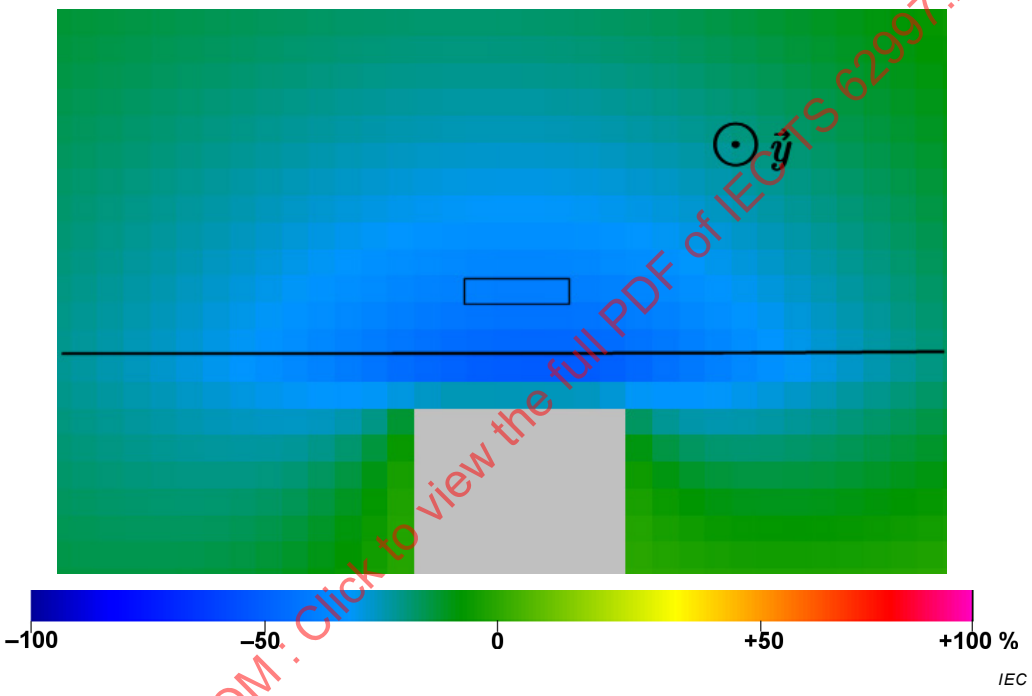

Figure F.8 – The local y-directed momentaneous maximal electric field pattern of the condition in Figure F.3, showing the 1 mm × 1 mm voxel size and the 5 mm^2 integration region 2 mm above the hand underside

The electric field distribution is more even in the hand side, so the averaged amplitude was only about 5 % less than that at the maximum point. The resulting average power density in the marked region in Figure F.8 and Figure F.9 was 0,263 W/dm^3, and corresponds to 80 % of the maximum point electric field maximum. The resulting quotient as obtained by comparative direct studies of the y-directed electric field pattern gave a reduction to 85 %. An average of 83 % resulted in the region nearest to the conductor.

The highest averaged maximum is thus at the hand side and not in the region very close to the conductor. The approximate value 0,325 W/dm^3 is therefore applicable for both the 2 mm and 4 mm hand above the coil.

Coupling value C_{coil} and CGCR data are listed in Clause G.3.

F.3 The hand model with tight fingers 6 mm above the coil and with variable position in the x direction – FDTD modelling

The distance a shown in Figure F.2 was –51 mm throughout in Clause F.2. It was now varied, with the distance z between the top of the coil and the hand model underside kept at 6 mm.

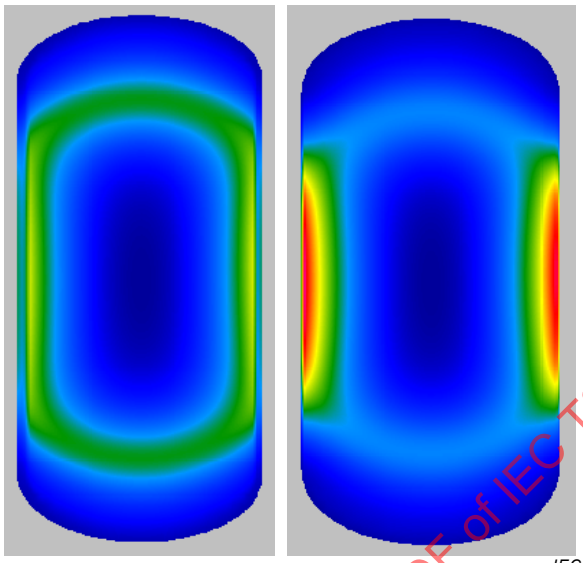

Figure F.9 – The power density pattern in the hand model centred above the coil and 6 mm above it; left image: bottom region, right image: 10 mm up

The colour scaling is the same in both images in Figure F.9. The numerical results and **CGCR** values for different distances a are given in Clause G.3.

F.4 The hand model with spread-out fingers, 6 mm straight above the coil – FDTD modelling

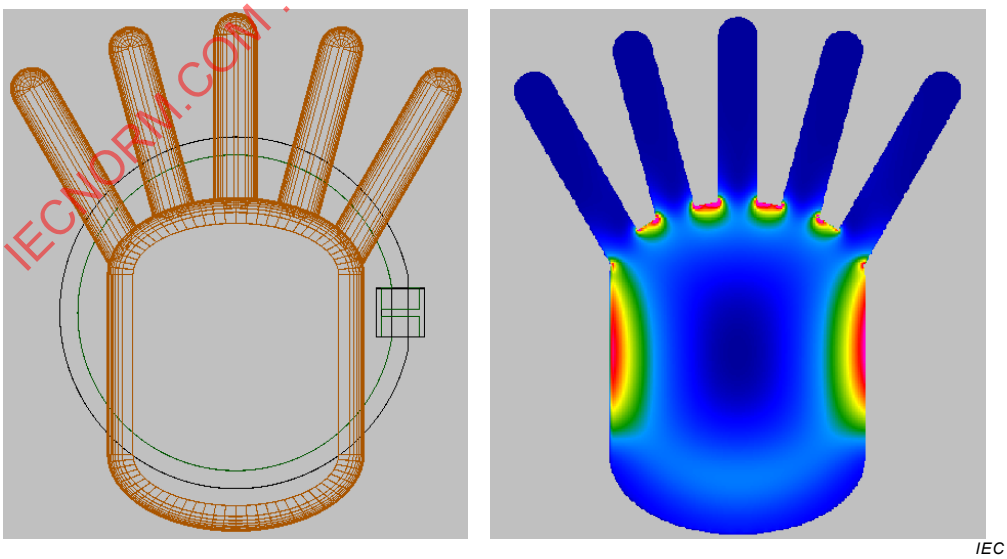

Figure F.10 – The hand model with spread-out fingers located 6 mm straight above the coil (left); relative power densities at the height of maximum power density between fingers (right)

The C_{coil} values were maximally at the hand sides were now about 0,33 m at 5 mm above the hand underside. The C_{coil} value at the inner ends of the fingers was maximally about 0,40 m, then 8 mm above the hand underside.

NOTE C_{coil} was 0,38 m in the centred (a = 0) case with tight fingers.

F.5 The hand model with tight fingers near a coil with metallic workload – FDTD modelling

The magnetic field and flux change with a highly conductive workload, due to the creation of eddy currents inducing a magnetic counterfield. Permeable metallic workloads will increase the magnetic flux and change its pattern.

NOTE Cases with magnetic circuits having a small opening between ends can substantially increase the magnetic flux. Due to the specific designs in such cases, only simple rod-shaped workloads in a coil are dealt with in this Technical Specification.

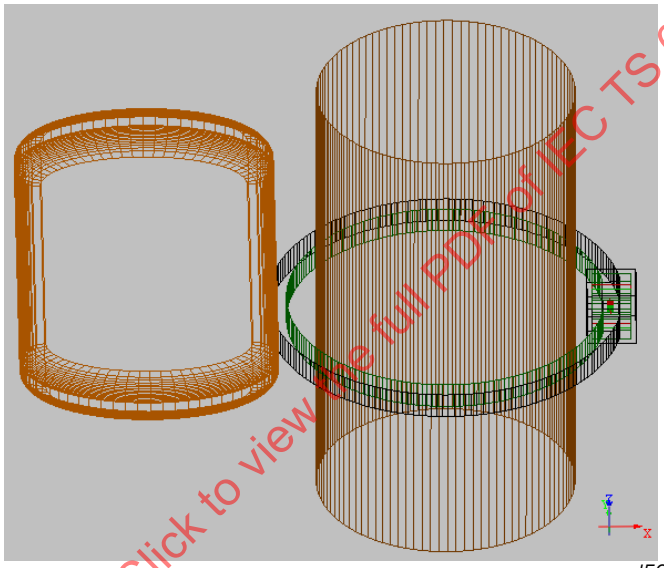

Figure F.11 – The hand model 6 mm above the coil and a 100 mm diameter metallic workload in the coil

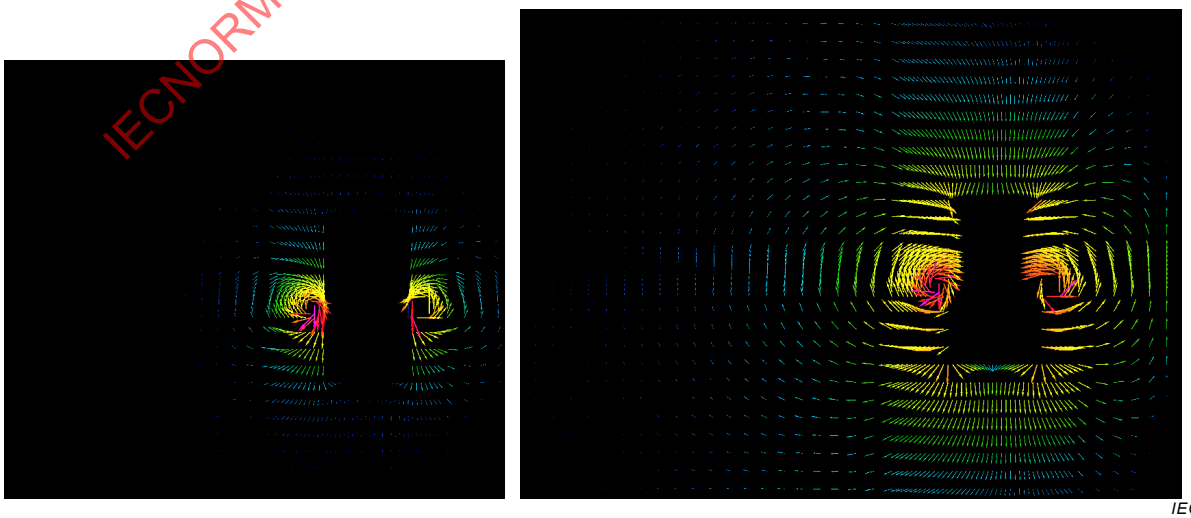

Figure F.12 – Quiver plot of the magnetic (H) field amplitude in logarithmic scaling, in the scenario in Figure F.11 with a non-magnetic (left) and magnetic (right) workload

Figure F.11 shows the scenario. The metallic workload has a conductivity of 4,2 × 10^5 Sm^{-1} in both cases in Figure F.12, and the workload in the right image also has a relative permeability μ = 1 000. The spread-out of the magnetic field is seen. The operating frequency is 6 MHz.

Figure F.13 shows the power density pattern in the hand model. Since the skin depth in the metal should be realistic for operating frequencies 5 kHz to 30 kHz, i.e. about 1 mm to 4 mm, the conductivity of the object was now set to about 600 Sm^{-1} , and μ to 200, still with the operating frequency 6 MHz. The C_{coil} value without the workload is 0,083 m, as listed in Figure G.2 for *a* = –110 mm as shown in Figure F.2. The pattern with the workloads is the same, but the C_{coil} value with both workloads is now only 0,066 m. However, the reduction with hand height shown in Figure G.1 will be less, since the magnetic field strength upwards remains higher. This is shown in Figure F.14. The colour scaling is different in the two images. The C_{coil} value is 0,014 m without the workload and 0,043 m with it, i.e. three times higher with the permeable metallic workload. There is thus no strong C_{coil} value reduction with hand height along the workload surface at this horizontal distance of 15 mm from the workload.

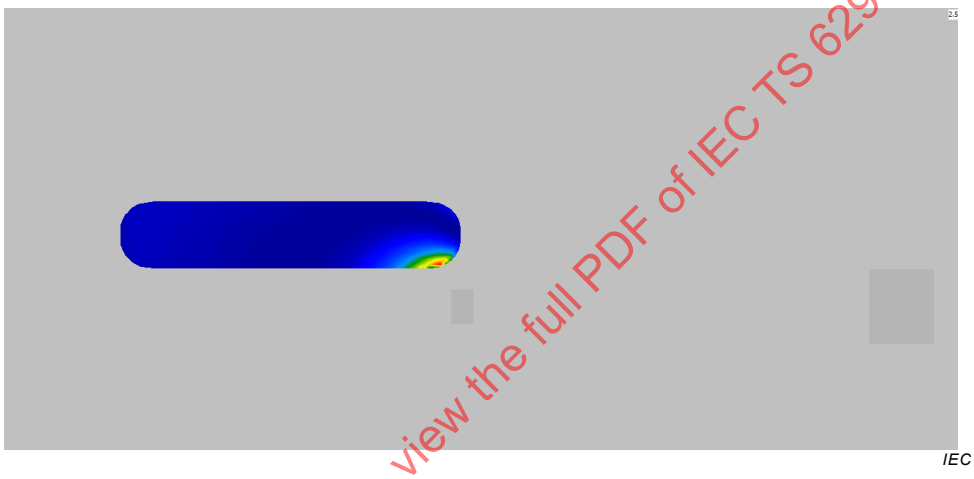

Figure F.13 – The power density pattern in the central vertical cross section in the hand scenario in Figure F.11

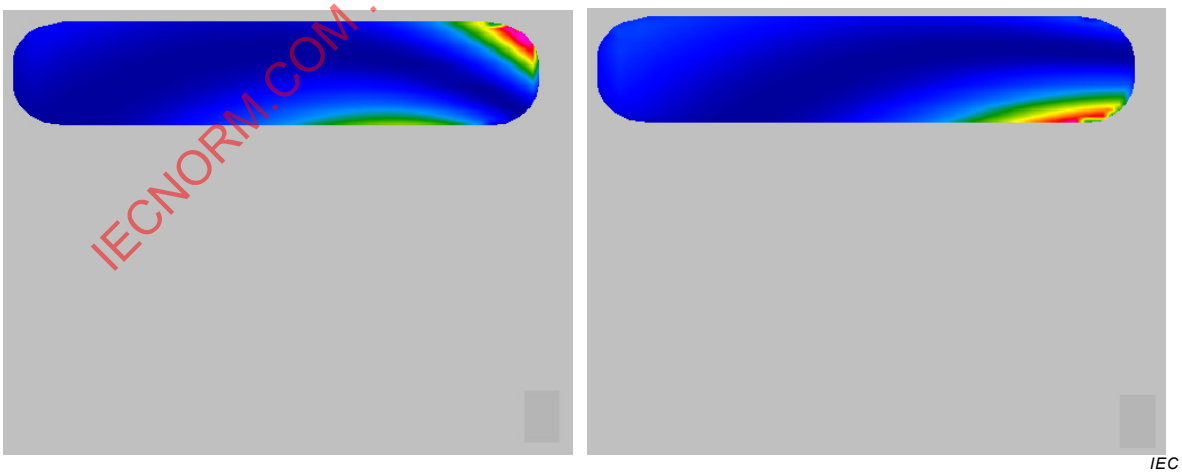

Figure F.14 – The power density in the central vertical cross section of the hand as in the scenario in Figure F.11, but 50 mm above the coil; with no workload (left) and with permeable metallic workload (right)

F.6 The finger model 2 mm above the coil – FDTD numerical modelling

F.6.1 The scenarios

The scenarios with two finger positions are shown in Figure F.15. The conductivity σ was set to 10 Sm^{-1}.

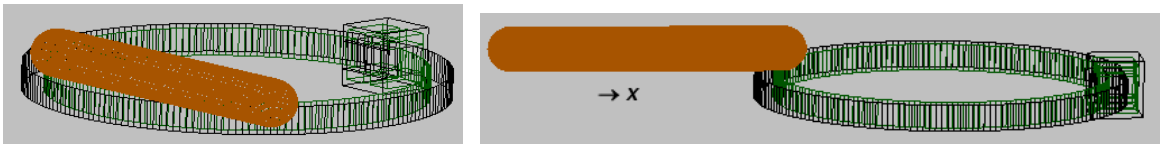

Figure F.15 – The two finger positions above the coil; left = y-directed finger

F.6.2 Modelling results

The power deposition pattern in the y-directed finger case is shown in Figure F.16.

The image on the right shows the detailed pattern in the ½ mm square voxels.

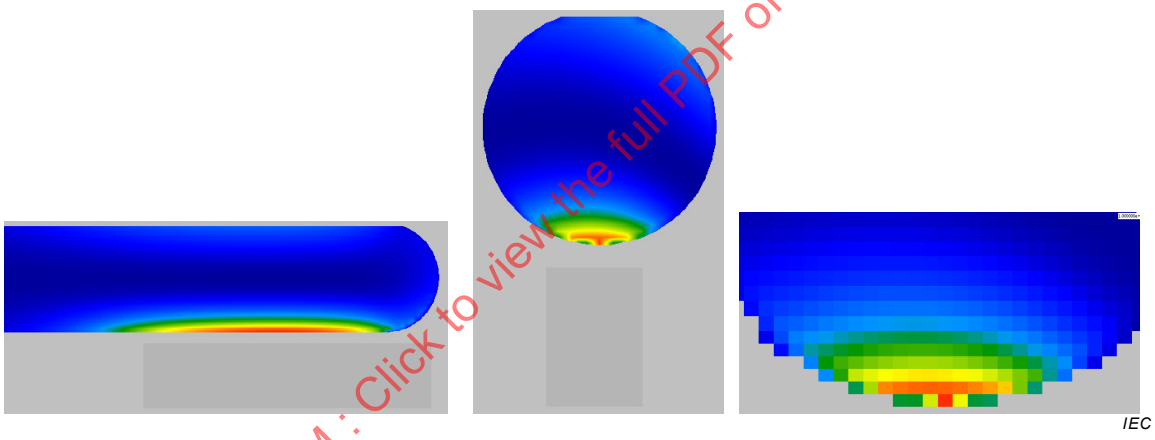

Figure F.16 – Power density maximum pattern in the y-directed 17 mm diameter finger model

The jaggedness is an artefact related to the unequal and displaced E- and H-voxels in FDTD scenarios. The power density in the dark orange voxels was 0,82 W/dm^3, 0,68 W/dm^3 in the yellow voxels and 0,60 W/dm^3 in the light green ones. This corresponds to C_{coil} values 0,095 m, 0,087 m and 0,081 m.

The power deposition pattern in the x-directed finger case is shown in Figure F.17.

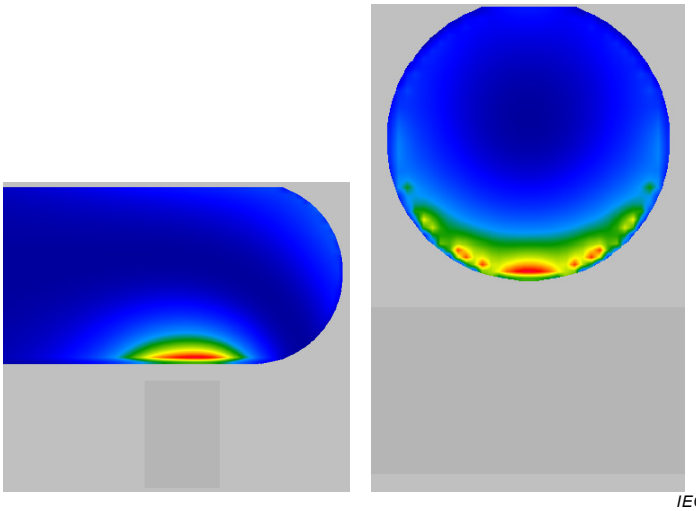

Figure F.17 – Power density maximum pattern in the x-directed 17 mm diameter finger model

The corresponding electric field deposition pattern is shown in Figure F.18.

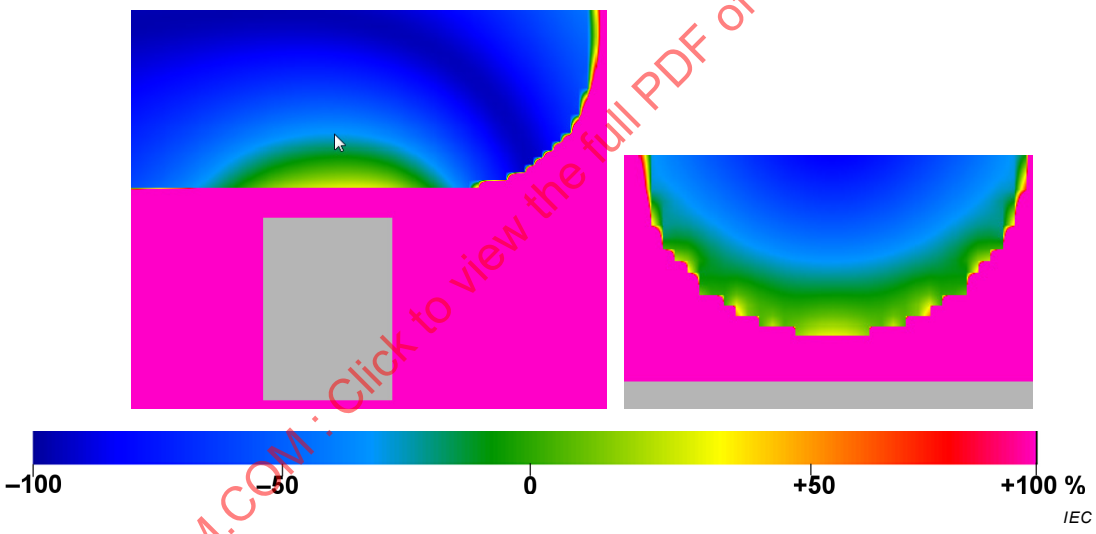

Figure F.18 – Momentaneous maximal electric field maximum pattern in the x-directed 17 mm diameter finger model

The jaggedness is now less pronounced. The maximum intensity (yellow) is 6,4 Vm^{-1} which corresponds to C_{coil} = 0,068 m. The intensity at the arrow in the left image, 3,0 mm up into the model, is 3,2 Vm^{-1}. This is consistent with the 5,5 Vm^{-1} obtained with the power density in a representative part.

F.7 Analysis of the FDTD modelling results

F.7.1 General

It is noted that the hand model position with the long side edge at the coil axis (x = –51 mm) is not the most onerous. The best conditions for creating a large circulating current flow, and by that the highest C_{coil} value, is with the hand centred over the coil, with the power density pattern shown in Figure F.9 (see Table G.2). Positioning the hand or finger radially outside and in the same plane as the coil plane results in a very significant reduction of the **coupling value** C_{coil} both since the intensity decay is larger there and since there is a tendency to a nullfield just outside the coil conductor, as for solenoids. It is also of interest that there will be no induced E field in the centre of a rotationally symmetrical object located anywhere at the same axis as that of the coil.

F.7.2 With the hand model

The difference between the two hand models is mainly by the increased density of the circulating current at the meeting ends of the fingers. Even if this is difficult to model with high accuracy due to the different kinds of tissue and the significant skin mass with a low conductivity, the induced electric field strength is typically not higher there than at the hand sides.

The overall modelling results clearly indicate that it is in practice meaningless to correlate the magnetic field amplitude at the strongest coupled regions to the induced electric field, for obtaining the C value. Instead, the axial magnetic field B_{coil} at the coil centre is a practically useful parameter.

The C_{coil} reduction with increasing axial distance from the coil of the hand centred straight above it is quite small. The induced E field is proportional to the square root of the power density, so there is no significant C_{coil} reduction from 2 mm to 4 mm distance. The reduction factor is only 3 (i.e. to about 0,020 m for the 50 mm distance). This is due to a compensation of the reduced magnetic field by its increasing curvature (i.e. smaller R_{osc}) as such providing an increased coupling. The same phenomenon also applies to the straight wire source; see Clauses E.5 and G.2.

F.7.3 With the finger model

The representative maximum E field strength is slightly smaller than that in the hand. There are two opposing reasons for this:

- the finger has a smaller curvature radius and cross section which reduces the C value in a homogeneous B field;
- there can no longer be such a strong oppositely directed current path as in the hand (see F.2.2); this results in an increased C value.

F.8 Volunteer studies

F.8.1 General

Volunteer studies were carried out with the coil in Figure F.1 and Figure F.2, with 11 kHz at 4,8 kA sinusoidal current. The coil was of course watercooled but still very warm, so a 2 mm opaque plastic plate was placed 1 mm above the top plane of the coil. This was also for preventing the volunteers from seeing the coil. For the blind testing, 7 points on the plate were marked with dots for finger/fingertop positioning and numbers for the records; see Figure F.19. Positions B and C were straight above the coil, and D at its axis. None of the four persons were able to sense anything at any position.

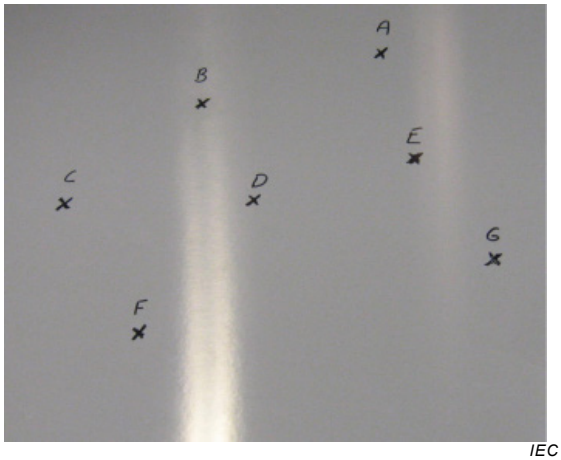

IEC

Figure F.19 – Plastic plate above the coil

In a second series of tests, the whole hand was placed flat on the plate, in different positions and with fingers tight and spread-out. It was now possible for all to perceive a tingling effect below the aversion level, in a part of the hand underside.

F.8.2 Calculations of the induced electric field strength in F.7.1

The C_{coil} rounded-off value 0,250 m obtained by numerical modelling with the hand model 2 mm to 4 mm above the top of the coil in the worst case, with coil average diameter 130 mm, Formula (B.3) and 4,8 kA RMS at 11 kHz is used. One then obtains B_{RMS} 46,4 mT; E_{RMS} 128V·m^{-1}.

Spread-out fingers in onerous geometry as in Clause F.4 can cause a very local C_{coil} value which is 50 % higher over a cross section of about 5 mm^2. The induced E field is then between perception and aversion, but over a very small region.

F.9 Comparisons with conventional electric shock effects by contact current

Finger impedances are quantified in the parallel Technical Specification IEC TS 62996. Using the perception current 5,9 mA at 11 kHz and the resulting impedance about 690 Ω, the voltage becomes about 4,0 V per finger. Supposing the finger length to be 10 cm, the electric field strength becomes 40 Vm^{-1}.

NOTE A typical male finger is longer and thicker than a female finger. The resulting impedance is therefore approximately the same.

Instead of using the **aversion** current 11 mA, the electric field strength becomes about 75 Vm^{-1}.